Kuhn, P. P., Echtler, H., Littke, R., Alfaro, G. (2010): Thermal basin modelling of the Arauco forearc basin, south central Chile — Heat flow and active margin tectonics. - Tectonophysics, 495, 1-2, 111-128

DOI: 10.1016/j.tecto.2009.07.026

Thermal Basin Modelling of the Arauco Forearc Basin, South Central Chile – Heat Flow and Active Margin Tectonics

Philipp P. Kuhn[a, b)], Helmut Echtler[a)], Ralf Littke[b)] + Guillermo Alfaro[c)]

Affiliations
a) GeoForschungsZentrum Potsdam, Telegrafenberg, 14473 Potsdam, Germany
b) Institute of Geology and Geochemistry of Petroleum and Coal, RWTH Aachen University, Aachen, Germany
c) Instituto de Geología Económica Aplicada, Universidad de Concepción, Concepción, Chile

(A) Abstract

The Arauco basin is part of the coastal forearc domain in South-Central Chile. During its evolution since the Late Cretaceous it was subject to multiple deposition cycles and the erosion of lower bathyal to beach and lagoon sediments. These different environments were established in alternating accretional and erosive subduction tectonic settings along the South Andean active margin. Whereas the general development is well understood, inconsistencies arise regarding the origin of the high thermal maturity of Eocene coals and the estimates of vertical movements of the whole area during the Cenozoic. Thermal modelling of this forearc basin provides new insights regarding its thermal evolution and evaluation of the magnitudes of subsidence and inversion. Results are based on the analysis of coal samples from surface outcrops, mines and drill cores of ten onshore wells from ENAP/Sipetrol. Newly derived vitrinite reflectance (VR_r) measurements indicated a temperature in the range of 135-150°C for the oldest sediment unit of the Arauco basin, which was reached in post Eocene times. Furthermore, 1D basin modelling techniques indicate scenarios that could explain the coalification values in the basin's sediments. The models were calibrated against VR_r data from drill core samples supplied by ENAP/Sipetrol. A Miocene and an Oligocene subsidence/inversion scenario were considered, while neither could be securely discarded based on the modelling results. Furthermore, it can be shown that the current thermal maturity was not reached by an increased heat flow (HF) or a deep subsidence only. Consequently, a structural inversion accompanied by the erosion of ~3.0±0.4 km depending on the locality in combination with a high HF of ~64±4 mW/m² is the best explanation of the available data. The HF, which is high for a forearc setting, can be attributed to the increased temperature of the relatively young subducted Nazca Plate and an additional influence of ascending hot fluids from the subduction zone. The maximum temperature gradient inferred is <30°C/km. Furthermore, the petroleum generation potential of the basin is considered to be rather low based on our results.

(A) Introduction

The Arauco forearc basin of south central Chile is situated in a rather cold active margin setting at the edge of the continental shelf close to the Chile-Peru-trench (Figure 1). Coals within the forearc basin sedimentary succession exhibit the highest thermal maturity of all Chilean coal (Helle *et al.*, 2000). However, there are only two published coalification values for the whole basin (Comisión-Nacional-de-Energía, 1989) and there were no previous models explaining the anomalously high coalification values in the Arauco basin, prompting this study.

The geological evolution of the Arauco basin started with the first deposition of Late Cretaceous shallow marine sediments on a crystalline Permo-Triassic basement (Figure 2). After alternating phases of uplift/erosion and subsidence/sedimentation, which are probably related to multiple cycles of accretion/erosion of the forearc wedge, a present maximum thickness of ~3000 m of sediment was deposited that varies dramatically along and across strike. Lower bathyal to beach and lagoonal sediments (Boettcher, 1999; Finger *et al.*, 2007; Mordojovich, 1981; Pineda, 1983) illustrate the range of geological environments the area underwent during the last 85 million years (Myr). Time gaps in deposition are discussed for four different periods and especially the development during the Oligocene, with a time gap of ~10 Myr is still uncertain.

Contradicting opinions, however, were published with respect to the timing of the maximum subsidence and thickness of now-eroded sediment layers during Neogene times. Melnick & Echtler (2006a) state a subsidence >1.5 km during Late Miocene for most of the segment between Juan Fernández Ridge to the Chile Rise (Figure 1) and a subsequent inversion since the Pliocene. Arguments for this uplift and inversion are based on tectonic, reflection seismic, stratigraphic and sedimentologic data (Encinas *et al.*, 2008; Finger *et al.*, 2007) related to the initiation of accretion, and thermochronologic data from fission track analysis (Glodny *et al.*, 2008) that argue for accelerated exhumation of basement during that time. The switch from a tectonic environment of subsidence and erosion to one of accretionary uplift followed the start of glacial denudation about 6 million years ago (Ma) (Melnick & Echtler, 2006a). Glacial denudation supplied the trench with a sufficient amount of sediments resulting in the subduction of water-rich material and thereby modifying the critical taper (Melnick & Echtler, 2006a). This tectonic history contrasts with a previous analysis, based on the interpretations of seismic profiles (Alvarez *et al.*, 2006) which proposed a moderate structural inversion about 10 Ma.

Fig. 1: The maps on the right show the location of the Arauco basin in its position east of the Peru-Chile Trench in the forearc of the South America Plate south of Concepción (Planiglobe, 2007); the left simplified geological map shows the main structures surrounding the emerged Arauco forearc basin (afterMelnick & Echtler, 2006b) together with the schematic profile indicating the elevation of the important features of the arc complex from the trench to the volcanic arc

Fig. 2: Generalized stratigraphy of preserved sediments in the Arauco basin based on well descriptions from ENAP using the International Geologic Time Scale after Gradstein *et al.* (2004); legend for sediment patterns is given in Figure 3

This study was designed to provide constraints on the thermal and burial history of 10 wells drilled by ENAP (Empresa Nacional del Petróleo, Chile) and our own collection of field samples and data which were the subject of 1D-modelling technique. The models presented are calibrated against new vitrinite random reflectance (VR_r) data that correlate to the maximum temperature to which the sediments were exposed (Taylor *et al.*, 1998). VR_r was determined for 31 drill core samples of ten exploration wells in the onshore part of the basin (Figure 3), which were provided by ENAP. Additional samples were taken from outcrops and mines across the Arauco Peninsula in order to provide a regional maturity data set on the Arauco basin. Special focus is set on the quantification of the magnitudes of vertical movements of the Arauco basin and heat flow (HF) evolution during the Tertiary.

Furthermore, the composition of the organic material in the sediments was analyzed to define the petroleum generation potential of all pre Miocene sediments to evaluate the petroleum generation potential of the survey area.

Fig. 3: Correlation of the major stratigraphic units of 9 of the sampled wells (supplied by ENAP) along the grey line in the small location map of the Arauco basin at the bottom. Light grey isolines show interpolated VR_r values based on new data derived from core samples.

(B) Geological Setting of the Arauco Basin

The Arauco basin (36°46’ to 38°30’ S) is situated in the coastal forearc domain of the Andean active margin of the South American Plate (Figure 1). About half of its 8000 km² (González, 1989) is represented by the offshore area that extends on the shelf of the continental margin. We focus on the onshore part with the

Arauco Peninsula, which was for a long period in the last century an area of extensive coal mining that served as the major national energy resource. Nowadays only a few mines are still operating, due to complex logistics related with faulting systems, seismic risks and thin coal seams that prevent cost efficient mining of the Early to Middle Eocene sub-/bituminous coals (González, 1989; Wenzel, 1969).

The long-term stationary position in an active forearc position (Echtler *et al.*, 2003; Glodny *et al.*, 2005) makes this onshore structure an outstanding and therefore an ideal target to investigate subduction processes and dynamics. The area of investigation is part of the south-central Chile subduction zone (36-39°S), situated in the Arauco-Nahuelbuta forearc block (Hackney *et al.*, 2006).

The Chile margin is formed by oblique subduction of the Nazca oceanic plate under the South American continent at a present day convergence rate of 66 mm/yr (Angermann *et al.*, 1999). The Arauco-Nahuelbuta forearc is located in the overlapping zone of the Valdivia 1960 (Mw 9.5 - Barrientos *et al.*, 2004) and Concepción 1835 (Mw ~8.5 - Lomnitz, 2004) mega-thrust earthquake segments. In this region, active crustal faults have been well mapped and described using coastal geomorphic features, seismic-reflection profiles, and microseismicity (Melnick *et al.*, 2006). These faults appear to be related to inherited ancient structures, which record the long term geological evolution of the margin. The morphotectonic segmentation of the Arauco-Nahuelbuta segment records pronounced, ongoing Quaternary uplift which appears to have persisted for a period of 10^6 years (Melnick *et al.*, 2009; Rehak *et al.*, 2008).

Based on apatite fission track (AFT) data, it appears that the entire Coastal Cordillera in the study area was eroded to crustal levels of about 3 km at ~70 ± Ma, i.e., in Upper Cretaceous times (Glodny *et al.*, 2008). The mainly Cenozoic evolution of the forearc domain is characterized by ‘breathing’-like oscillations of changing subduction geometry and fore arc thickness, possibly correlated with episodic changes between accretion and tectonic erosion (Bangs & Cande, 1997).

The general setting of the Andean forearc region appears to be remarkably stable, which rules out any large-scale, long-term continuous basal underplating, accretion, trench-parallel tilting, or tectonic erosion processes in the time interval between the Late Cretaceous and the Late Miocene. The Cordillera Nahuelbuta segment (~37°–38°S) of the Coastal Cordillera and the immediate substratum of the Arauco basin (Figure 1) experienced a distinct uplift and erosion episode from Pliocene to Recent time, as is evident from forearc tectonics (Melnick *et al.*, 2006; Melnick & Echtler, 2006a), morphometry (Rehak *et al.*, 2008) and thermal history models constrained by AFT data (Glodny *et al.*, 2008). Regional uplift in Plio-Pleistocene times in the 37°S–38°S forearc segment is further indicated by the emergence of the Arauco Peninsula.

As described previously (Encinas *et al.*, 2008; García, 1968; Glodny *et al.*, 2006; Pineda, 1983; Radic *et al.*, 2006) the development of the Arauco forearc basin (Figure 2) is generally agreed to have occurred during four different phases of sedimentation:

- The oldest sedimentary unit in the forearc basin was deposited during Late Cretaceous times (Santonian – Maastrichtian) in an extensional setting that is indicated by normal faults (Wenzel, 1972). Thicknesses range from 300 to 1300m.

- The second unit is dated to be Eocene to Early Oligocene. These rocks were deposited during a phase of active tectonic subsidence. The coal-bearing Trihueco and Curanilahue Formation indicate relative sea level changes during that period (Wenzel *et al.*, 1975). After the deposition of the Late Eocene Millongue Formation no further record of the Oligocene is preserved. This gap can either be explained by a time of geological quiescence or by a complete cycle of deposition and subsequent total erosion of sediments. Neither alternative has been constrained by geological archives.

- After an erosional event, Miocene sediments were deposited as the third sequence. The Ranquil Formation, which is 100 - 390 meters thick, is composed of marine sediments of shelf, slope and lower bathyal depositional environments. The Formation is truncated at the top by a major discontinuity that is interpreted to be indicative of a major structural inversion during the Middle Pliocene.

- The Tubul formation of the Plio- Pleistocene was deposited locally in subsiding areas that coexisted with areas of uplift and deformation. All clastic sediments of the Arauco basin are to some degree influenced and displaced by supra-curstal normal faults whereas the the peninsula is characterized by a NW-SE-oriented active anticline due to ongoing upper plate contraction (Melnick *et al.*, 2009). The main direction of the faulting inherited from older structures strikes NE and divides the study area into numerous smaller blocks tilted mainly to the west.

The morphology of the peninsula is described from west to east by: the uplifted coastal area from the northern Punta Lavapié to the southern area around Lebu; a lower region in the centre from Arauco to the area of Cañete; and the higher elevation in the east at the foothills of the Coastal Cordillera.

(A) Samples

Eighty Cretaceous to Miocene rock samples provide new thermal maturity data that is representative of the stratigraphic succession throughout the Arauco basin. VR_r was measured on samples from ten onshore exploration wells drilled between 1968 and 1973 (Figure 3), which were provided by ENAP (Empresa Nacional del Petróleo, Chile) from the company core store in Santiago, Chile. Only thirty-one of the core samples taken from ten onshore wells were feasible for vitrinite reflectance measurements. Additional samples were taken from outcrops and mines across the Arauco Peninsula, in order to provide a regional thermal maturity data set for the Arauco basin. Four samples are from two active coal mines (CARVILE, Lebu and Enarcar, Trongol/Curanilahue) and the rest was collected from surface outcrops across the peninsula during a field mapping program in spring 2006.

An attempt was made to sample all the Formations occurring in the basin. Unfortunately, only very few Neogene samples could be taken. Furthermore, the pre-Cretaceous rocks (metamorphic Basement), proved to be insufficient for VRr measurements due to low content of organic matter.

(A) Methods

To evaluate Arauco basin's thermal history this study focuses on the maximum paleo-temperature recorded by thermal maturity indicators in sedimentary rocks. Random vitrinite reflectance (VR_r) is the primary thermal maturity indicator used to infer maximum temperatures during burial (Barker & Pawlewicz, 1993; Lopatin, 1971; Sweeney & Burnham, 1990). VRr measurements were performed on all samples containing coal or organic matter. Additionally, the content of organic carbon and petroleum generation potential were assessed using Rock-Eval pyrolysis. T_{max} values obtained by this method can also indicate organic thermal maturity and maximum paleo-temperatures based on correlations between VR_r and T_{max} (Espitalié, 1986; Leckie *et al.*, 1988; Rullkötter *et al.*, 1988; Teichmüller & Durand, 1983).

(B) Vitrinite Reflectance

Vitrinite is the coal maceral group most often used for reflectance measurements due to its relatively progressive change in optical properties with increasing maximum temperature. It is a reliable parameter that can be used to calibrate the thermal history of sedimentary basin models. For these measurements polished sections of coal or sediments containing dispersed organic matter (DOM) were prepared and the reflectance of vitrinites in randomly orientated positions was measured following established procedures (Stach *et al.*, 1982;

Taylor *et al.*, 1998). The data obtained were measured using a Zeiss Axioplan microscope equipped with the DISKUS Fossil (Technisches Büro Carl H. Hilgers) software using an isotropic yttrium-aluminium-garnet isotropic standard (R_r = 0.889%).

Random vitrinite reflectance measured on DOM usually differs from observed values taken from coal samples of equivalent maturity rank. In particular $VR_{r\ measured\ on\ DOM\ are\ typically\ more\ scattered}$ (Scheidt & Littke, 1989). The greater dispersion of observed VR_r values can be attributed to several factors, including allochthonous vitrinites of higher maturity, measurements of inertinite that could not be distinguished from vitrinite, and artefacts due to small particle size or the quality of the polished surface (Senglaub *et al.*, 2006).

(B) Pyrolysis

Total organic carbon (TOC) for most samples was analysed by using a LECO RC-412 Multiphase Carbon Determinator. Rock-Eval bulk pyrolysis (Espitalié *et al.*, 1977) was performed on a number of samples to characterise the petroleum generation potential and residual potential of the source rocks. When combining results from TOC measurements and Rock-Eval bulk pyrolysis the Oxygen Index (OI) and the Hydrogen Index (HI) can be calculated, these are usually plotted against each other in a pseudo-van Krevelen diagram to determine the kerogen type of the analysed material analogue to the original van Krevelen diagram (Espitalié *et al.*, 1977; Tissot & Welte, 1984; vanKrevelen, 1961).

(B) 1D Basin Models

Geohistory diagrams (Van Hinte, 1978) and similar diagrams have been widely used in geology, particular in hydrocarbon exploration. Lopatin (1971), Waples (1980), and Welte & Yükler (1981) adapted these diagrams to perform numerical modelling of burial, erosion and thermal histories in sedimentary basins. This method has become an important tool in the search for new petroleum plays or for the evaluation of exploitable oil and gas accumulations around the world.

For this study only selected wells were modelled using PetroMod1D (version 10.0 SP1) software of IES, Aachen, Germany, since some wells were only sampled over a very narrow depth range. Due to the limited amount of available data a two dimensional model was not attempted. The combined stratigraphic and thermal paleo-history of the modelled wells were calibrated against the observed VR_r dataset that was specifically obtained for this study. The EASY%Ro kinetic algorithm (Sweeney & Burnham, 1990) was used to calculate the model VR_r values inferred for each model. The recent HF was determined by the temperature gradient that

could be calculated from a limited number of well temperature measurements. Models were constructed to illustrate the last 85 Myr of the geological history. An additional 15 km of basement material was added obligatorily at the base of all models to buffer the heat flow, whose source was expected to be located below the model. The value of 15 km is only an approximation based on the TIPTEQ seismic line (Micksch, 2008) south of the research area and does not represent the actual distance to the subduction zone.

The preserved stratigraphic succession provides information on deposition, non-deposition or erosion, on which the models are based. Greater uncertainties are associated with the time intervals for which no rock record are preserved, specifically weather those intervals are represented by an erosional unconformity, or hiatus in deposition (Wheeler, 1958). Absolute ages were attributed using the published time scale of Gradstein *et al. (*2004). Lacking specific lithological and material parameters for the rock units used in the models we employed average rock compositions constrained by well descriptions and field data. Combinations of default lithological and material parameters values provided by the PetroMod software were applied in the model.

Boundary conditions like paleo-water depth (PWD) and sediment water interface temperature were inferred. Based on the stable location in the structural setting above the subduction zone throughout the evolution of the basin, in the first models a time invariant heat flow (HF) history was used. Later the HF scenarios were adjusted to reach the maturities that are indicated by VRr data and the present well temperatures measured in the boreholes.

The 1D models were employed to predict maximum temperature and its duration during burial. By varying the less constrained geohistory parameters it was possible to fit model thermal maturity indicators through iterative calibration of models to the observed VR_r values. The analysis produces a range of possible burial history scenarios, which provide valuable input to further discussion on basin evolution. The concept of numerical basin modelling calibrated by vitrinite reflectance data is explained in more detail by Senglaub et al. (2006).

(A) Results and Discussion

(B) Analytical Results

(C) Vitrinite Reflectance

The deepest strata show highest thermal maturity values (Quiriquina $VR_{r\ max}$ = 1.00%) while samples from shallower units produce the lowest thermal maturity values (Ranquil $VR_{r\ min}$ = 0.41%). The results are in same range as the two previous published data points from the Comisión Nacional de Energía (1989) of 0.64 ± 0.07%. As displayed in Table 1 the VR_r for core samples range from 0.61 to 1.00% and are usually a little higher than those from coal samples from the same stratum from outcrops or coal mines. Standard deviations (SD) of the reflectance measurements in this study are mostly below 0.06%.

Using the classification scheme proposed by Teichmüller (1987), the coal rank of all samples ranges from Sub- to High Volatile Bituminous. While most of the well samples can be inferred from their VRr and Tmax to have entered the oil window, only a few samples have experienced temperatures commonly associated with "peak oil generation" or higher values (Baskin, 1997; Taylor *et al.*, 1998). Even though the coals indicate even lower maturity indicators they might have just entered the oil generation threshold, since they are comparable in their composition to coals in New Zealand (Sykes & Snowdon, 2001).

A plot of VR_r against depth (Figure 4A) exhibits a quite similar trend in almost all the wells with more than two samples. Additionally, when converting VR_r into temperatures with use of the formula

$$T_{peak} = (\ln (VR_r) + 1.68) / 0.0124 \qquad \text{(}\textit{Formula 1}\text{ - Barker \& Pawlewicz, 1993)}$$

the higher values suggest a maximum temperature of ~135°C, assuming any time dependence is negligible. By plotting these calculated temperatures against depth (Figure 4B), temperature gradients for the time of the highest temperatures in the basin can be calculated, assuming that peak thermal maturities were obtained simultaneously in response to sedimentary burial. The inferred paleo-geothermal gradients range from 17.6 to 26.8°C/km with most clustering around 26°C/km. When considering the influence of time, higher temperature/-gradient have to be considered when the duration of the highest heat flow is not continuous.

These values are lower than the general global average 30°C/km geothermal gradient for continental crust, as might be expected for a forearc setting. However, they are high for a forearc setting (Lutz *et al.*, 2004). Rather

unexpected is that the gradients are ~15°C/km lower than recent measurements taken at ODP Sites 1233 (41°S), 1234, and 1235 (both ~36°20' S) on the shelf of the South American continental upper plate (Grevemeyer *et al.*, 2003).

The current temperature gradient, based on temperature measurements in six exploration wells located in the Arauco basin, was averaged to be at 16°C/km. Therefore, a significant change of the temperature gradient during the development of the basin sediments has to be proposed.

With the knowledge of the paleo-geothermal gradient it is possible to make initial evaluations of the burial depth. The simplification used in *Formula 1* and the approximation of a linear geothermal gradient enable the estimation of eroded section:

$$((T_{\text{depth h}} - 10\ [°C]) / T_{\text{grad}}\ [°C\ km^{-1}]) - h\ [km] = Inv\ [km] \qquad \textit{(Formula 2)}$$

with $T_{depth\ h}$ as maximum temperature at a certain depth (from VR_r with *Formula 1*), minus 10°C representing approximate surface temperature, T_{grad} as the calculated temperature gradient, *h* as the depth for which the maximum temperature was calculated, and *Inv* as the amount of eroded section estimated for the basin in this position. For example inferred paleo-geothermal gradient of 26°C/km and a maximum temperature of 125°C at 1.65 km depth suggests that ~2.8 km of sedimentary succession has been eroded from the section.

Further conclusions can be drawn from the derived VR_r data when normalizing the depth of each sample to "Penhue 1" well (Figure 4C), which was picked as standard because of its almost complete stratigraphic column. Hence all VR_r data points were plotted according to their stratigraphic position in their respective formations relative to the corresponding depth of the same formation in the "Penhue 1" well. All wells, with the exception of the "Curanilahue 2" and "Rio Trongol 1" wells, have similar relationships between stratigraphic position and themal maturity to that observed in the "Penhue 1" well (Figure 4C). Furthermore, data points from wells "Lebu 1", "-4", and "-6", which have only single thermal maturity observations are also in agreement to the general relationship between stratigraphic position and thermal maturity illustrated by "Penhue 1" well. Even more striking are the indications of an almost uniform temperature history for the Arauco Peninsula shown by the absence of discontinuities in the thermal maturity profiles, while the inferred paleo-geothermal gradients are largely linear for all the drill core samples. This permits to infer confidently that it is correct to assume that the maximum temperature was reached simultaneously in response to sedimentary burial after the deposition of the Millongue Formation in the Late Eocene during the last ~30 Myr.

When comparing the stratigraphy of the 9 wells with interpolated VR_r data in Figure 3, a slight correlation of the VRr data with the stratigraphy is observable. It is further notable that the southern wells were probably hotter than the “Curanilahue1”, “Tubul Este 1” and “Tubul 1” wells. Wells “Rio Trongol 1” and “Curanilahue 1” are situated in the eastern part of the basin. Both seem to have been buried to similar depth, but they appear to have preserved a thermal history record indicating a greater eroded thickness, based on interpretations of Figure 3. Similar elevated inversion might also be the reason for the higher VRr at shallower depth in “Lebu 5”.

Fig. 4: Graph A indicates the VR_r data against depth of all wells with data at more than one measured depth point; when using Formula 1 together with the data in A it is possible to define the temperature gradients during a long termed temperature maximum in the basins sediment as displayed in Graph B. Graph C shows the VR_r data measured on drill core samples of nine wells of the Arauco basin. The data of eight wells are standardised to their stratigraphic position to the well “Penhue 1”. The displayed data of the wells fit well with a linear gradient and therefore suggest a similar temperature history. Since the overall trend does not show significant anomalies in any direction, it can be concluded that the maximum temperature event occurred after the youngest of the measured samples was deposited. Since the youngest drill core sample on which VR_r was measured is from the Millongue Formation (Upper Eocene), an Upper Eocene or younger maximum temperature event is evident.

(C) Rock-Eval Pyrolysis

The samples analyzed using Rock-Eval pyrolysis can be subdivided into three groups based on TOC values. Some are samples from the surface area (including coal mines), which show TOC values generally higher than 50% and up to 78%. Unfortunately no cores of these coaly strata were retrieved from any of the sampled wells. This does not indicate that these stratums are not available in the location of the well, but that either these sections were not cored or sample material from these intervals is no longer available from these wells. In contrast to the high TOC coal, samples from the metamorphic basement have TOC contents of less than 0.06%, which makes them unsuitable for this study. The third group, from the other sedimentary lithologies, has intermediate TOC values. As shown in Table 2 most of the samples from drill cores belong to this group. They average ~1.4% TOC. Five of these samples have TOC higher than 2% and more than half of these samples have values greater 0.5%, which could be sufficient to be a hydrocarbon source rock, albeit a lean and

gas-prone (i.e. HI < 200 mg HC / g TOC). Unfortunately, it was not possible to sample a sufficient amount of the rock column to comment definitely on the petroleum potential of the basin, and inferences can only be made based on sampled strata.

The content of inorganic carbon in all samples is quite low with an average of 0.2% and a maximum of 2.4% for 50 analysed samples.

Results from the Rock-Eval measurements are plotted in Figure 5 as HI vs. OI and show two major data clusters, representing two different groups of organic material. The group with low OI and HI values from 150 to 400 mg HC/g TOC comprises almost all the coal samples that were analysed. Values above 300 mg HC/g TOC are rather high for Type III kerogen (Tissot & Welte, 1984), but this might be explained by deposition in a paralic-coal-forming environment (Amijaya & Littke, 2006) and similar coal from the New Zealand area (Sykes & Snowdon, 2001). The second major cluster extends parallel to the OI axis and comprises almost all samples taken from the wells at all depths. It is evident that deeper units tend to have lower OI values, probably related to higher temperatures in the past that resulted in CO_2 generation and expulsion. The youngest greater subsequent erosional event and cooling of the succession terminated petroleum generation reactions. The rest of the samples have either a very low initial hydrocarbon potential (high OI and low HI → immature) or reached temperatures high enough for the process of oil and gas generation and expulsion to deplete any remaining hydrocarbon potential (low OI and low HI → mature).

The Rock-Eval pyrolysis parameter that indicates the thermal maturity is T_{max} [°C] with values <430 for the immature stage, 430 to 435 for the beginning of petroleum formation, 435 to 450 for peak oil generation, and >460°C for the post oil generation stage (Baskin, 1997). The measured values are displayed in Table 2. The T_{max} values are plotted against the corresponding VR_r values in Figure 6 and show a reasonable consistency for the total data set. Furthermore it is evident that the coals, the samples with the highest HI, might have just entered the generation window during times of maximum temperatures in the study area.

The results show that maturity levels indicative of petroleum generation existed only in the deepest and oldest units in the basin. While the coals seem to be less matured by the temperature they must have experience, the dispersed organic material found in the cores seems to have reached the mid mature stage even in the Trihueco Formation (Fig. 6. - 0.6% VRr, (Baskin, 1997; Tissot & Welte, 1984)). However, the oil and gas potentials of the drill core samples of the area are inferred to be low due to the low TOC and HI readings on available

samples. In contrast to this, the potential for oil generation by the coals seems to be more promising. The Tmax and VRr have reached the rank threshold for oil generation defined by Sykes & Snowdon (2001).

Fig. 5: Pseudo-Van-Krevelen-Type-Diagram with HI and OI from Table 2 of all Arauco Peninsula samples tested. The clustering of the coal samples parallel to the HI axis is similar to Cretaceous and Paleogene coals in New Zealand and South-East Asia.

Fig. 6: Plot of VR_r (Table 1) versus T_{max} (Table 2) shows reasonable correlation between both thermal maturity indicators. Superimposed are values from Leckie *et al.* (1988), the Posidonia Shale taken form Rullkötter *et al.* (1988) and a worldwide database (Petersen, 2006) for comparison.

(B) Numerical Basin Modelling

(C) Setup of 1D PetroMod Model

The models of the wells, which are based on known geological events, are calibrated against the newly derived thermal maturity data described above. Some additional constraints that contribute to the development of conceptual models and boundary conditions for the 1D models are summarized and discussed below.

(D) Boundary Conditions

Tectonic processes which could influence the development of the Arauco basin are identified in Figure 7. It is not possible to include all processes that may influence the model of this study. While a selection of processes with an indirect impact are displayed (Figure 7), processes with possible strong impact are discussed below. The knowledge and understanding of these processes is incorporated into the derivation of suitable boundary processes required as input to the models.

Fig. 7: Tectonics that influence the development of the basin, which need to be incorporated into the conceptual model. A indicates the convergence velocity of the Nazca Plate and the South American Continent in the last 40 Myr, while B depicts the internal development stages of the basin (both based on Melnick & Echtler, 2006a, and references within).

(D) Paleo Water Depth (PWD)

The PWD is usually determined by combination of tectonic subsidence and changes in global sea levels. A local PWD model was derived considering sedimentological models using well descriptions by ENAP and a publication by Pineda (1983). For some Neogene sediments the data presented by Finger *et al.* (2007) and Nielsen & Glodny (2006) were incorporated. Deep bathyal environments during the Upper Miocene (Finger *et al.*, 2007) are not used in this study, since a shallower water depth is expected in the western part of the basin, which are farther away from the trench.

(D) Sediment Water Interface Temperature

The sediment water interface temperature was modified from a PetroMod internal dataset based on Wygrala (1989). Cooler temperatures were introduced when deeper water depths were used in the models. The variation during the last 50 Myr is around 8°C, which has minor effects on the temperature gradient in the shallower sediment units.

(D) Heat Flow

The heat flow (HF) of a basin in a forearc position is usually expected to be rather low. This is due to the subduction of the heavier oceanic crust underneath the lighter continental plate. Since the top of the oceanic crust together with its overlying sediments is generally cooler than the lower parts of the continental plate, the cooler subducted areas "suck" the heat out of there surrounding environment till a new equilibrium is reached. This results in lower temperature gradient in the forearc location, where e.g. the Arauco basin is located. Good illustrations of heat flow profiles across the whole arc profile can be found in Hyndman *et al.* (2005).

This is in agreement with the temperature measurements that were available for six wells in the area. Unfortunately, these were not always the wells for which vitrinite reflectance data is available – an average temperature gradient was derived to determine the recent heat flow of ~35 mW/m² for Arauco basin. Since it is impossible to explain the maturity of the organic material with this low heat flow and a reasonable subsidence and inversion history without reaching average velocities > 2mm/yr in the limited time frames that allow such movements, the heat flow throughout the evolution of the basin has to be considered as variable. Therefore, an above average heat flow is assumed for the forearc of the Arauco basin during its evolution.

Periods of increased heat flow are not unusual in this setting (Hyndman *et al.*, 2005) and even common in the outer forearc (Dählmann & de Lange, 2003; Hensen *et al.*, 2004). In the worldwide dataset collected by Hyndman *et al.* (2005) it is visible that the HF values in front of the arc are below ~ 50 mW/m² but increases up to 80 mW/m² in direction of the subduction zone. Individual higher values ~90 mW/m² are reported for the Ryukyu forearc region and of ~100 mW/m² for the Central Andes (Hyndman *et al.* 2005 and references within). Even in-situ values of >100 mW/m² for the forearc region of the Central Andes were published (Grevemeyer *et al.*, 2006). The maximum HF in the past can be evaluated with the use of basin modelling techniques as described above. However, since thermal maturity data are primarily influenced by the time of maximum temperatures, the temporal variations of the thermal history cannot be inferred reliably for other time with lower temperature conditions. In such cases, the thermal history must be inferred from analogues based on similar tectonic processes. Since no other data for the Arauco basin were accessible, paleo HF estimates were constrained by the observed thermal maturity of samples, while the measured well temperatures were used for the recent HF.

(D) Conceptual Model

The greatest challenge for the thermal modelling of the Arauco basin is to define the timing of the expected major subsidence during the post-Eocene. Since not enough reliable maturity data for the younger formations could be retrieved that would hint at a linear continuation or a jump in maturity after the Oligocene sediment gap, a secure statement can not be given. When constructing the conceptual model each event of sedimentation whether it is later eroded or still available in the basin needs an assigned rock lithology with corresponding parameters. Physical rock parameters were defined using composed default values as discussed previously (Table 3).

The following uncertainties should be considered when reviewing the models: [1.] The lithological compositions of each formation are expected to actually be variable in vertical and lateral directions. [2.] The default values used in the model may not represent the actually deposited rocks. [3.] The rock composition estimated from well descriptions may be inaccurate. Nevertheless, considering the available data, this is the most appropriate approach to derive an acceptable range of physical rock properties without actually measuring physical properties of each core sample.

The essential part of the conceptual model is the evolution of the basin in terms of kinematics. Due to the uncertainties related to most important events, a number of diverse scenarios were constructed and modelled.

The timing of the major subsidence phase with a related structural inversion and erosion of more than 2 km is fundamental. Possible time frames are the Oligocene related to the gap in the sediment record of ~10 Myr, or the Late Miocene uplift and erosion following major subsidence. One example of a conceptual model setup based on the latter, including ages of erosion and deposition, is described in Table 4. Naturally, the amount of erosion can vary from one well position to the other, especially after major structural inversion and erosion when locally different amounts of underlying Eocene are deformed, exposed and denuded, or preserved. Therefore, the conceptual model may be adjusted for other wells, depending on the preserved sediments and the assumed tectonic processes. Figure 8 displays the data from Table 4 for “Penhue 1” well model as a schematic illustration from the time of the first deposition to Recent times. The source of the heat is expected to be located underneath the basin, therefore an additionally basement of 15 km has been added underneath the basin sediments of each conceptual model to act as a thermal buffer with its heat capacity due to the great volume of rock. The basement does not include a radiogenic heat source, since Gamma Ray readings in wells that reached the basement showed very low values for the bedrock.

Fig. 8: Graphic presentation of the conceptual models for well “Penhue 1” for the Miocene subsidence scenario described in Table 4; A includes the PWD while only the rock column is displayed in B. Calculated VRR values are indicated in B.

(C) **Results from the 1D modelling**

Thermal maturity models were developed to account for all known parameters and assumptions described above, and constrained with thermal maturity and well temperature data. Parameters that were varying were those exerting first order influence on thermal development like maximum burial and basal HF. These were adjusted iteratively to get the best possible fit to constraints. During the modelling it became obvious that varying only single model input data would not provide an acceptable fit. Consequently a number of different combinations of parameters, such as the maximum subsidence, or the variation of the maximum heat flow values and its length were considered in numerous model iterations to determine the scenario with the best fit to the thermal maturity data.

Stratigraphic consistency of thermal maturation indicators suggested the uniform development of the research area in response to a similar maximum burial event. Therefore a single well model that resulted in a good fit to the data could be used as a template for all the other well models with slight modifications to reach a similar fit to the calibration data in each well. Therefore, in the following only the "Penhue 1" well is used as an illustrative example, since it has a large number of thermal maturity sample data points with a good fit to the numerical model predictions (Figure 9).

Fig. 9: VR_r data fit of the Oligocene (structural inversion and erosion 3120 m and HF of 64.7 mW/m²) and Miocene (3100 m and 64.5 mW/m²) structural inversion and erosion model using the conceptual model described in Table 4 (modifications were made for the Oligocene scenario).

As mentioned above a major phase of subsidence followed by structural inversion and erosion has to be considered in the model. However, both - the Oligocene and the Miocene - structural inversion and erosion scenarios provide a good fit to the available calibration data (Figure 9). Note that a fit to data within an Oligocene erosion scenario requests an estimated structural inversion and erosion of 3120 m and a HF of 64.7 mW/m², and best fit to a Miocene erosion scenario requires an inversion of 3100 m and 64.5 mW/m². Therefore, neither of the scenarios can be discarded based on these model results.

(D) Maximum Subsidence in Relation to Maximum Heat Flow

The amount of subsidence and subsequent structural inversion and erosion necessary to explain the coalification of the sample locations is a key concern of this analysis. Previous work and analysis had inferred that a subsidence >1.5 km during the Late Miocene (Encinas *et al.*, 2008; Finger *et al.*, 2007) and temperature

of up to 100°C in Eocene coals. Furthermore, Glodny *et al.* (2008) assumed a maximum erosion of 3 km since Upper Cretaceous time for the nearby Coastal Cordillera, which can be used as an indication for the possible amplitude of vertical movement in the greater Arauco area.

Considering the above, the amount of burial was assessed and probable basin development models were created (Figure 10). To simplify matters in the following discussion only the Miocene scenario is described, since the results are transferable to the Oligocene scenario. Additionally, alternative "extreme" models were based on the assumption [1] of deep burial of the basin sediments with low HF or [2] high HF with less burial. For the first case [1] an erosion of 4400 m paired with a low HF of 54.5 mW/m² would still give a reasonably good fit to the observed data. The other extreme model [2] that still showed an adequate fit with the calibration data was defined by a cover of just 1850 m of additional sediment together with a HF of 74.5 mW/m². The most suitable version for "Penhue 1" was found in the combination of 64.5 mW/m² HF and uplift/erosion of 3.1 km when the model's output agreed best with the calibration data gradient and most data points.

The described best fit relation of HF and structural inversion and erosion rate were further tested on all wells with two or more thermal maturity measurements, since it is expected, based on the VR_r data, that the complete basin developed in a uniform way. HF values between 60.5 and 66.5 mW/m² and erosion rates from 2600 to 3350 m were required for best fit to calibration data. The HF-structural inversion and erosion combinations are displayed in Figure 11 for each well with two or more VRr measurements.

Fig. 10: Different results for modelling approaches for "Penhue 1" with different HF values and the structural inversion and erosion combination as displayed in Figure 11

Fig. 11: Diamond shape symbols show different combinations of HF values and the structural inversion and erosion required for the most reasonable fit with calibration data set of "Penhue 1" as displayed in Figure 10; circles indicate best fit models for all tested wells with two or more calibration points

Finally, during the development of all scenarios it was always considered that sedimentation and erosion should not exceed values above 1.4 mm/yr. It is expected that subsidence, structural inversion and erosion did not occur at steady rate over the complete time span, but over short intervals at irregular rates, possibly connected to earthquakes, and at some times at very slow or negligible rates.

When constructing the conceptual models some assumptions had to be made to develop a consistent basin evolution model.

For the Oligocene subsidence scenarios, there are only a few parameters that have to be considered. The fact that there is no sediment record for this time in the study area permits the construction of several different plausible models for the time interval between 33 and 23 Ma.

When building the conceptual models for the Miocene subsidence scenario an assumption had to be made for sediments that were assigned to the "Ranquil (Navidad)" in the original well descriptions of well "Penhue 1" and "Tubul 1". Since these persisting volumes of rock are considered to be part of the sediment column that was deposited during time of the major subsidence, and have therefore been overlain by a considerable column of sediment (> 1km), they can not be assigned to the only weakly lithified Late Miocene "Ranquil (Navidad)" Formation. Therefore, these sediments are considered to have accumulated in the Early-Middle Miocene already and are referred to as "LowMio" (*Low*er *Mio*cene) in the Miocene subsidence scenario.

Fig. 12: Stratigraphic correlation of the formations in wells drilled on Isla Mocha by ENAP

(C) Discussion of 1D Modelling

During iterative model development for different heat flow and subsidence scenarios it emerged that neither deep subsidence nor an increased HF, alone, could explain the measured thermal maturity values in the Arauco basin. A combination of both burial and increase HF results in the best data fit at all depths. From the geological and paleontological data there are two time windows at which the maximum burial could have been reached. Subsidence and subsequent uplift and erosion could have taken place during the Oligocene or the Late Miocene to Middle Pliocene. Both time intervals are in agreement with the newly derived VR_r data that suggest a post Eocene event. However, it is not possible to eliminate one possibility based solely on the basin modelling results. Therefore other evidence needs to be found if these two alternatives are to be distinguished.

(D) The Oligocene scenario

For the ca. 10 Myr during the Oligocene (33.9 – 23.03 Ma) no sediment deposition is reported either in the wells used in this study or in any other part of the basin as described by several studies (González, 1989; Pineda, 1983). It can either be presumed that this is a time of geological quiescence or minor erosion (Finger

et al., 2007). A different scenario could be that all earlier deposited Oligocene units were completely eroded in a major erosion event, which accompanied subsequent uplift of the area. This would further explain the erosive truncation of all Eocene formations that is seen in outcrops and wells. A hypothetical reason why reworked Oligocene rocks have not yet been identified could be that most of them were carried over the edge of the shelf and further downslope into the trench area, where they eventually became subject to subduction. However, the suggestion of major subsidence during the Oligocene remains speculative.

The models predict a structural inversion of ~3.1 km together with a long term HF of 64.7 mW/m² for the Oligocene scenario to explain the high coalification of the Eocene coals.

(D) The Miocene Scenario

If the required major subsidence occurred during the Miocene then the following limits on the timing of events need to be considered. The youngest Miocene nearshore deposition in the Arauco basin occurred 16.1 Ma (Nielsen & Glodny, 2006). Furthermore, a prominent structural inversion of >1.5 km of the study area is described by Melnick & Echtler (2006a) for the Middle Pliocene and supported by FT data in the Coastal Cordillera (Glodny *et al.*, 2008) which was also uplifted during the Pliocene. This allows a time window for the subsidence of almost 11 Myr from ~15.5 to 4.5 Ma during which an almost bathyal environment has to be assumed to be present for sometime between 10 and 4.5 Ma according to Finger *et al.* (2007). This water depth is not used in any of the models since the sampling location which is closest to any of the wells (LMB from Finger *et al.*, 2007) shows only one species indicating water depth of 1500 to 4000 m, while all other fossils from the wells are described to be indicative of 500 to 1500 m maximum water depth. Since the wells that are considered in this study are situate further away from the subduction zone and in a more proximate location to the sediment source in the west, than described locations in the Finger *et al.* 2007 publication, for this study it is expected that the water depth in the models should not exceed a maximum depth of much more than 1000 m.

Considering the above described constraints, the successive development of the basin for the Miocene scenario is modelled as follows (Table 4): The layers of the LowMio Formation are considered to be remnants of thicker Early Miocene successions deposited in nearshore environments. This starts with beach sediments that changed to finer grained depositions due to increasing water depth, while sedimentation continued because of increasing slope angles that developed from the east of the basin close to the continental sediment source. During continued subsidence with an increase of slope angles slope apron sediments like turbidites and sandy debris flow units developed (Encinas *et al.*, 2008). After several Myr subsidence slowed and finally stopped

with sediment filling the newly generated accommodation space. The maximum water depth (described by PWD in the well models) should have varied through time, laterally from west to east across peninsula, since the sediment input is expected to derive from the continent in the east. These sediments, deposited in the area of the Arauco Peninsula, are then eroded probably related to the structural inversion mainly during Pliocene proposed by Melnick & Echtler (2006a).

The sediments which have been eroded from the peninsula during the structural inversion and related erosion should be similar to the Miocene sediments found on Isla Mocha ~30 km to the west. Sánchez (2004) interpreted these sediments to be turbidites and wells by ENAP showed thicknesses of Miocene rocks up to 924 m (Figure 12; Mocha Norte 1) with an erosional unconformity at the surface. Therefore, even greater thicknesses may have been present. Furthermore, Miocene sediment thickness variations are in the range of ~500 m over a distance of 10 km on Isla Mocha (Figure 12).

(D) Evaluation of Model Scenarios

The model in which the necessary subsidence/structural inversion history that is outlined above, is developed with the necessary sediment cover and heat flow needed to fit the observed thermal maturation of analysed samples and bore hole temperatures and is the simplest scenario in which the high coalification could have developed without invoking any as yet unspecified events.

As seen from the description above there are no reasons to eliminate either of the proposed models. The 1D basin modelling produced that the best calibration data fit in all wells, even with different timings (Oligocene or Miocene), were usually reached by an erosion of 3170 ±450 m with a maximum HF of 69 ±2 mW/m². All average sedimentation rates used in the models are kept below 1 mm/yr, while some erosion values are higher, especially in the “extreme” subsidence/inversion scenario models. These values are considered to be reasonable for the Arauco basin area and its regional setting based on available data.

However, when comparing both scenarios with each other, further pros and cons were considered to determine the geological development, which best explains the Arauco basin.

The problem with the Oligocene subsidence/erosion scenario is the lack of confirmation in the preserved sediment record. With no stratigraphic constraints, anything could have happened, but nothing can be constrained using preserved information (Figure 13). The only tectonical event that might give a possible reason for a distinct change in the basin development might be the change in plate convergence rate that falls within this time window (Figure 7). Advantages in the Miocene subsidence/erosion scenario are the presence

of preserved sediment records, which indicate that there was subsidence and deposition during this period. Miocene sediment thicknesses in the Mocha area suggest the probability of a great thickness of coeval sediment (960 m - “Mocha Este 1”) and subsequent erosion, since other Mocha localities have only 450 m of Miocene formations (“Mocha Norte 1”). There are rapid variations in the thickness of the Miocene succession over distances of ~10 km. Additionally, the uplift of the greater shelf area (Finger *et al.*, 2007) and the bordering Coastal Cordillera (Glodny *et al.*, 2008) in the Pliocene are consistent with the Miocene subsidence/Pliocene inversion scenario.

Based on all available information and due to the very reasonable fit of the Miocene model to newly derived findings on the geological development of the greater area, the scenario including a Miocene subsidence with a Middle Pliocene inversion of ~3.0 ±0.4 km currently is preferred (Figure 13).

Finally, even slower, long-term exhumation rates of 0.6 ±0.2 mm/yr of the Coastal Cordillera throughout the Cenozoic (2008) are not in conflict with the presented models, since the shelf might have interacted more directly with subduction zone and accretion wedge events. Nevertheless, the proposed inversion of the Arauco basin reaches values up to 1.4 mm/yr. The suggested amount for vertical movement might still be to low to be detected by the fission track method used by Glodny *et al.* (2008) since low temperature gradients exist in the sediment succession in the basin. Therefore, the relatively high HF for the forearc setting of Arauco basin has to be proposed.

Fig. 13: Possible development of the subsidence and inversion history of the Arauco basin is displayed for the Miocene inversion scenario by the black line. The diagonally striped areas represent the PWD through time. Areas of unavailable sediment record in the greater area are marked by lighter areas in the bottom part of the figure. For these times the dashed grey lines represent possible scenarios how the basement –sediment contact could have developed; greater and lesser vertical movements are described. The grey line represents the Eocene coal layer from which several samples were derived.

(C) **Maximum Heat flow**

During numerical basin modelling various scenarios were tested in which the temperature of the sediments at certain times in the past reaches values that explain the thermal maturity of the analysed drill core samples. The temperatures could not be attained based solely on sensible subsidence and the related additional sediment cover together with an average HF estimated for forearcs (Allen & Allen, 2005), therefore an increased HF has to be considered. As discussed earlier, values up to 80 mW/m² are still in the range for the forearc setting (Hyndman *et al.*, 2005, and references within), while values up to 100 mW/m² (Grevemeyer *et al.*, 2006; Hyndman *et al.*, 2005) are probably exceptions and confined locally. Also in the bordering Coastal Cordillera, which is also part of the forearc, a fairly "normal" geothermal gradient around 30°/km is suggested (Hamza & Munoz, 1996). Therefore the increased HF used to obtain best results during numerical modelling is still rather high for a forearc setting, but not impossible when reasonably connected to potential sources.

Some sources like friction induced heat (Lutz *et al.*, 2004), radiogenic heat, or exothermic metamorphism could be eliminated for the area of the Arauco basin along with the impact of any external heat source. Influence of volcanic activity or other short timed heat impacts can also be discarded. Conducted models with the impact of high (~ 100 mW/m²) short heat pulses shorter than 5 Myr could not reproduce an acceptable fit with the calibration data when the heat source was expected to be located underneath the 15 km of basement.

(D) Hydrothermal Influence

The impact of ascending hot fluids from the subduction zone is quite reasonable in a setting where large amounts of water saturated ocean sediment are subducted and later dewatered by tectonic compression or incorporation into the accretionary prism and low-grade metamorphic reaction. Dewatering and related heat transfer is most likely possible near the base of the accretionary complex (Fisher & Hounslow, 1990; Foucher *et al.*, 1990). The rise of the fluids from the subduction zone into the forearc wedge is probably triggered by earthquakes (Husen & Kissling, 2001) which are abundant in the arc region. Possible dewatering paths are explained in more detail by Grevemeyer *et al.* (2006).

Further support for this possibility of increased HF is that the proposed temperatures are still in a relatively low range of ~135°C (when expecting a shorter heat pulse temperatures of ~150°C are needed - Barker & Pawlewicz, 1993) at the bottom of the Arauco basin. This range of temperatures can be reached by over-pressured fluids even after rising through parts the upper plate. In similar subduction zone settings the development of fluids with temperatures of 85 - 165°C was described (Dählmann & de Lange, 2003; Hensen *et al.*, 2004). Oleskevich *et al.* (1999) even narrow down the temperature range to 100 - 150°C for accretionary

related subduction zones in which further fluids are generated by the dehydration of smectite clays. Finally, it has to be added that these are not constant flows, but local peak-like anomalies (Grevemeyer *et al.*, 2003), which can enable heat flow values up to 140 mW/m² (Grevemeyer *et al.*, 2006). While the existence of these fluid flows from the subduction zone can be assumed (Grevemeyer *et al.*, 2006) the volume, and therefore the lateral impact, is still subject of discussion. Wang *et al.* (1993) calculated that the increase related to ascending fluids on the heat flow at the toe of an accretionary prism should be in the range of an additional 10%.

(D) Heat of the Subducted Plate

Increased temperature of the relatively young subducted Nazca Plate could also be responsible for a high HF. According to the empirically derived formula by Parsons and Sclater (1977)

$$HF\ [mW/m^2] = 473 / t^{1/2} \qquad 0 < t < 120\ Myr \qquad \textit{(Formula 3)}$$

a HF of more than 60 mW/m² from the subducted oceanic crust can be expected if an age of 60 Myr is used for the calculation. The subduction of oceanic crust with ages of 60 Myr and younger is quite reasonable according to plate movement velocities for the area by Parado-Casas & Molnar (1987). Even younger ages can be expected when using recent plate movement velocities (Kendrick *et al.*, 2003) and ocean plate ages by Müller *et al.* (1997). Of course some of this energy is used to increase the temperature in subducted sediments and to reach temperature equilibrium in the lower crust. Still, a long lasting high HF from the subduction zone through the accretionary wedge to the bottom of the basin sediments is a possible consequence.

(D) Discussion on Heat Flow

The impact of ascending hot fluids from the subduction zone appears to be quite reasonable. The assumption that large amounts of water-saturated sea sediments are subducted and used as material for accretion is supported by the occurrence of calcite veins in fractured Cenozoic stratums which confirm the existence of fluid flow in the basin sediments. Less information is found on the actual path of the fluids through the forearc, which allows speculations on either vertical flow from deeper regions or more lateral flow from shallower regions of the subduction zone. The vertical path version can be supported by Melnick *et al.* (2006) who show the relation of earthquake locations with fracture zones in the forearc and its basin. Fluid flow might have been triggered by earthquakes, which pressed the fluids out of the pores while the fracture zone, which stretch from the subduction channel to the upper part of the plate, were used as pathways.

Unfortunately, the cooling rate of the fluids when travelling from the base of the continental crust to the base of the basin sediments is high (Wang *et al.*, 1993) and therefore the effect does not reach the surface with its full extend. Still, as Wang et al. (1993) showed for accretionary prisms, if good permeability, possibly due to fracturing resulting from ongoing deformation in the active margin setting, exists an increase of heat flow by 10% at the toe of the accretionary wedge could be possible. Further insecurities arise when discussing the length and number of these hydrothermally induced heat pulses. Can they be expected to be continuous since the subduction zone incorporates water on a regular basis, which might be expelled permanently, or are there multiple events of high temperature peaks occurring sporadically, whereas the basement has enough volume (heat capacity) to buffer the impact to a minimal increase? As seen during the modelling, a single short term extremely high heat pulse can probably be disregarded as an explanation of the existing maturity since this would not fit the calibration data.

The other plausible theory is a longer lasting higher HF induced by the subducted young and therefore hotter oceanic Nazca plate. Of course, this theory introduces questions on how well the paleo-temperature can be defined by using the method by Parsons & Sclater (1977 - *Formula 3*) based only on the age of oceanic plate in the past, which is a matter of further speculation. However, an increase of HF in comparison to the "normal" subduction zone due to the subduction of a younger oceanic plate could give a very relevant explanation for the setting of the Chile-Peru Trench in the region of the Central Andes.

While discussing the HF it has to be kept in mind that only the value for the time of maximum temperature (either the Oligocene or the late Miocene) can be derived from modelling, since VR_r is mainly affected by the highest temperature during burial. Therefore, periods in which the temperature is more than 20 – 30°C below the maximum temperature are not influencing the reflectivity of the vitrinites in any recordable manner (Barker & Pawlewicz, 1993; Burnham & Sweeney, 1989). Hence, the quantified maturation was reached during a single event of subsidence with coexisting high HF, which has to be considered for the temperature modelling.

In summary, the HF of 64.4 ± 4 mW/m² has to be assumed which is higher than the average HF in forearc basins varying from 20 to 45 with a mean 35 mW/m² (Allen & Allen, 2005). Higher HF induced by the subducted young oceanic plate that is amplified by fluids ascending through fracture zones from the subduction zone might be a possible explanation for the increased values. The persisting challenge will be to quantify the relative impacts of the different sources, which is beyond the scope of this study.

(B) Discussion of modelling results

While developing a numerical model as described in the previous paragraph a great number of uncertainties have to be discussed and evaluated. Major variables that influence the basin model are related to petrophysical properties of the basin's sediments, mode of heat transfer, calibration data and the algorithm for the vitrinite reflectance data.

During this study it was not possible to measure the thermal conductivity or heat capacity of the basin sediments due to sparse sample material. Therefore, these values were quantified for all formations by combinations of default rock property data with respect to well descriptions. Since a large percentage of the formations consist of sand and clay, the variations seem to be in an acceptable range. Of greater uncertainty are the properties of eroded formations.

Of course the quality of the VR_r data, which is used for calibration of all models, needs to be addressed. Since most of the measurements were confirmed by repetition, because of the low SD and rather high number of sample points, an excellent data quality can be expected. Furthermore, the good correlation with the T_{max} data and the similarity with already published data (Comisión-Nacional-de-Energía, 1989) support the high data quality.

Another uncertainty is related to the algorithm used to calculate vitrinite reflectance. The equation by Sweeney & Burnham (1990) which was used here is regarded as state-of-the-art and has been often adopted for the maturity range found in the Arauco basin.

For further and more detailed information on the uncertainties in basin modelling see Senglaub *et al.* (2006).

(A) Conclusions

Based on newly derived maturity data (vitrinite reflectance; T_{max} of Rock-Eval pyrolysis) from samples taken on the surface, in mines, and wells of the Arauco basin it was possible to define a maximum temperature of ~135 - 150°C reached at the base of the basement-sediment contact during its development during post Eocene times, depending on a constant or shorter termed maximum temperature in the forearc wedge, respectively.

In correlation with available data, possible time windows for maximum temperatures are discussed, i.) during Oligocene characterized by a sedimentary time gap or ii.) during Middle Miocene to Middle Pliocene. It emerged that the second option is in agreement with

a) a sub-bathyal environment during Late Miocene that provides the needed accumulation space for a thick sediment cover

b) a >1.5 km basin inversion and pronounced uplift since Pliocene from the stratigraphy

c) up to 960 m of Miocene sediments found on Isla Mocha which are interpreted to be turbidites sourced from the basin inversion to the east

d) a distinct uplift and exhumation episode in Pliocene to Recent time derived from apatite fission track data for the eastern region of the Coastal Cordillera

In contrast, the Oligocene time span is neither constrained by a reliable sedimentary record nor any regional signal of subsidence and inversion.

1D models based on ENAP wells calibrated with VR_r data emphasize a subsidence and subsequent uplift and erosion of ~3.0 km together with a long term heat flow (HF) up to ~64.4 mW/m². A temperature gradient of <30°C/km at the time of maximum temperature is estimated. The increased temperature of the relatively young subducted oceanic plate is probably the reason for the increase in HF, which was enhanced by the impact of ascending hot fluids from the subduction zone via fracture zones that are described for the area. Other possible influences like radiogenic or frictional heat are negligible for the studied area.

All modelled wells had a good fit with the calibration data to the thermal regime and the basin evolution is assumed to be relatively uniform across the region of interest.

The rather low modelled temperature history suggests a thermally immature basin with limited petroleum generation potential. Only the available coal layers have a considerable potential for oil generation.

(A) Acknowledgements

We thank Lisandro Rojas from ENAP for permission and access to the core material and well descriptions and Pamela Alvarez , Daniel Melnick, Charlotte Krawczyk, and Charlotte Cederbom for help and discussions.

Very special thanks to the GEA of the Universidad de Concepción staff for hosting and supporting P. Kuhn during his stay in Concepción and during field work. We also thank the mining company Carbonifera Victoria de Lebu S.A. for supporting sampling. We would like to thank Rob Funnell and an anonymous Reviewer for there constructive reviews that help improve the manuscript and Richard Sykes for valuable additional comments. The studies and field work in Chile were financed by DAAD, RWTH Aachen and GFZ Potsdam.

(A) References

Allen, P.A., Allen, J.R., (2005) *Basin analysis: principles and applications*. Blackwell Publishing, Oxford.

Alvarez, P., Radic, J.P., Rojas, L., (2006) Evolucion Tectonosedimentaria de la Cuenca de Antearco Arauco Itata, Chile Central. In: *XI Congreso Geológico Chileno*, Antofagasta, Chile.

Amijaya, H., Littke, R., (2006) Properties of thermally metamorphosed coal from Tanjung Enim Area, South Sumatra Basin, Indonesia with special reference to the coalification path of macerals. *International Journal of Coal Geology*, 66(4), 271-295.

Angermann, D., Klotz, J., Reigber, C., (1999) Space-geodetic estimation of the Nazca-South America Euler vector. *Earth and Planetary Science Letters*, 171(3), 329-334.

Bangs, N.L., Cande, S.C., (1997) Episodic development of a convergent margin inferred from structures and processes along the southern Chile margin. *Tectonics*, 16(3), 489-503.

Barker, C., Pawlewicz, M.J., (1993) Calculation of Vitrinite Reflectance from Thermal Histories and Peak Temperatures. A comparison of methods, *ACS Symposium Series (1994)*, pp. 216-229. American Chemical Society, Washington, DC.

Barrientos, S., Vera, E., Alvarado, P., Monfret, T., (2004) Crustal seismicity in central Chile. *Journal of South American Earth Sciences*, 16(8), 759-768.

Baskin, D.K., (1997) Atomic H/C ratio of kerogen as an estimate of thermal maturity and organic matter conversion. *AAPG Bulletin*, 81(9), 1437-1450.

Boettcher, M., (1999) Tektonik der Halbinsel Arauco und angrenzender Forearc-Bereiche (südliches Zentral-Chile). In: *Paläontologischen Institutes*. Universität Hamburg, Hamburg.

Burnham, A.K., Sweeney, J.J., (1989) A chemical kinetic model of vitrinite maturation and reflectance. *Geochimica et Cosmochimica Acta*, 53(10), 2649-2657.

Comisión-Nacional-de-Energía, (1989) *El sector energía en Chile*. Comisión Nacional de Energía, Santiago, Chile.

Dählmann, A., de Lange, G.J., (2003) Fluid-sediment interactions at Eastern Mediterranean mud volcanoes: a stable isotope study from ODP Leg 160. *Earth and Planetary Science Letters*, 212(3-4), 377-391.

Echtler, H.P., Glodny, J., Gräfe, K., Rosenau, M., Melnick, D., Seifert, W., Vietor, T., (2003) Active tectonics controlled by inherited structures in the long-term stationary and non-plateau south–central Andes. In: *EGU/AGU Joint Assembly*, Nice.

Encinas, A., Finger, K.L., Nielsen, S.N., Lavenu, A., Buatois, L.A., Peterson, D.E., Le Roux, J.P., (2008) Rapid and major coastal subsidence during the late Miocene in south-central Chile. *Journal of South American Earth Sciences*, 25(2), 157-175.

Espitalié, J., (1986) Use of Tmax as a maturation index for different types of organic matter. Comparison with vitrinite reflectance. In: J. Burrus (Ed.), *Thermal modeling in sedimentary basins* (Ed. by J. Burrus), pp. 475-496. Editions Technip, Paris.

Espitalié, J., Laporte, J.L., Madec, M., Marquis, F., Leplat, P., Paulet, J., Boutefeu, A., (1977) Methode rapide de caracterisation des roches meres de leur potentiel petrolier et de leur degre d'evolution. *Revue de l'Institute Francais du Petrole*, 32, 23-42.

Finger, K.L., Nielsen, S.N., Devries, T.J., Encinas, A., Peterson, D.E., (2007) Paleontologic Evidence for Sedimentary Displacement in Neogene Forearc Basins of Central Chile. *Palaios*, 22(1), 3-16.

Fisher, A.T., Hounslow, M.W., (1990) Transient fluid flow through the toe of the Barbados accretionary complex; constraints from Ocean Drilling Program Leg 110 heat flow studies and simple models. *Journal of Geophysical Research*, 95(B6), 8845-8858.

Foucher, J., LePichon, X., Lallemant, S., Hobart, M., Henry, P., Benedetti, M., Westbrook, G., Langseth, M., (1990) Heat Flow, Tectonics, and Fluid Circulation at the Toe of the Barbados Ridge Accretionary Prism. *J. Geophys. Res.*, 95(B6), 8859-8867.

García, F., (1968) Estratigrafía del Terciario del Chile Cenral. Empresa Nacional del Petróle, Santiago, Chile.

Glodny, J., Echtler, H., Figueroa, O., Franz, G., Gräfe, K., Kemnitz, H., Kramer, W., Krawczyk, C., Lohrmann, J., Lucassen, F., Melnick, D., Rosenau, M., Seifert, W., (2006) Long-Term Geological Evolution and Mass-Flow Balance of the South-Central Andes. In: O. Oncken, G. Chong, G. Franz, P. Giese, H.-J. Götze, V.A. Ramos, M. Strecker, P. Wigger (Eds.), *The Andes—Active subduction orogeny*, *Frontiers in Earth Sciences* (Ed. by O. Oncken, G. Chong, G. Franz, P. Giese, H.-J. Götze, V.A. Ramos, M. Strecker, P. Wigger), pp. 355-375. Springer-Verlag, Berlin Heidelberg New York.

Glodny, J., Grafe, K., Echtler, H., Rosenau, M., (2008) Mesozoic to Quaternary continental margin dynamics in South-Central Chile (36-42 degrees S): the apatite and zircon fission track perspective. *International Journal of Earth Sciences*, 97(6), 1271-1291.

Glodny, J., Lohrmann, J., Echtler, H., Grafe, K., Seifert, W., Collao, S., Figueroa, O., (2005) Internal dynamics of a paleoaccretionary wedge: insights from combined isotope tectonochronology and sandbox modelling of the South-Central Chilean forearc. *Earth and Planetary Science Letters*, 231(1-2), 23-39.

González, E., (1989) Hydrocarbon resources in the coastal zone of Chile In: G.E. Ericksen, M.T. Cañas Pinochet, J.A. Reinemund (Eds.), *Geology of the Andes and its relation to hydrocarbon and energy resources; Circum-Pacific Council for Energy and Hydrothermal Resources*, *11* (Ed. by G.E. Ericksen, M.T. Cañas Pinochet, J.A. Reinemund), pp. 383-404. Circum-Pacific Council for Energy and Mineral Resources, Houston, Texas.

Gradstein, F.M., Ogg, J.G., Smith, A.G., (2004) *A Geologic Time Scale 2004*. Cambridge University Press, Cambridge, United Kingdom.

Grevemeyer, I., Diaz-Naveas, J.L., Ranero, C.R., Villinger, H.W., (2003) Heat flow over the descending Nazca plate in central Chile, 32[degree sign]S to 41[degree sign]S: observations from ODP Leg 202 and the occurrence of natural gas hydrates. *Earth and Planetary Science Letters*, 213(3-4), 285-298.

Grevemeyer, I., Kaul, N., Diaz-Naveas, L, J., (2006) Geothermal evidence for fluid flow through the gas hydrate stability field off central Chile; transient flow related to large subduction zone earthquakes? *Geophysical Journal International*, 166(1), 461-468.

Hackney, R., Echtler, H., Franz, G., Götze, H.J., Lucassen, F., Marchenko, D., Melnick, D., Meyer, U., Schmidt, S., Alasonati-Tašárová, Z., Tassara, A., Wienecke, S., (2006) The Segmented Overriding Plate and Coupling at the South-Central Chilean Margin (36–42° S). In: O. Oncken, G. Chong, G. Franz, P. Giese, H.-J. Götze, V.A. Ramos, M. Strecker, P. Wigger (Eds.), *The Andes—Active subduction orogeny*, *Frontiers in Earth Sciences* (Ed. by O. Oncken, G. Chong, G. Franz, P. Giese, H.-J. Götze, V.A. Ramos, M. Strecker, P. Wigger), pp. 355-375. Springer-Verlag, Berlin Heidelberg New York.

Hamza, V.M., Munoz, M., (1996) Heat flow map of South America. *Geothermics*, 25(6), 599-646.

Helle, S., Alfaro, G., Kelm, U., Tascon, J.M.D., (2000) Mineralogical and chemical characterisation of coals from Southern Chile. *International Journal of Coal Geology*, 44(1), 85-94.

Hensen, C., Wallmann, K., Schmidt, M., Ranero, C.R., Suess, E., (2004) Fluid expulsion related to mud extrusion off Costa Rica; a window to the subducting slab. *Geology (Boulder)*, 32(2), 201-204.

Husen, S., Kissling, E., (2001) Postseismic fluid flow after the large subduction earthquake of Antofagasta, Chile. *Geology (Boulder)*, 29(9), 847-850.

Hyndman, R.D., Currie, C.A., Mazzotti, S.P., (2005) Subduction zone backarcs, mobile belts, and orogenic heat. *GSA Today*, 15(2), 4-10.
Kendrick, E., Bevis, M., Smalley, R., Brooks, B., Vargas, R.B., Lauria, E., Fortes, L.P.S., (2003) The Nazca-South America Euler vector and its rate of change. *Journal of South American Earth Sciences*, 16(2), 125-131.
Kuhn, P.P., (2007) Thermal Modelling of a Cenozoic Forearc Basin at the Active Continental Margin of South America: Coalification and Sedimentology of the Arauco Basin, Chile. In: *LEK*, pp. 65. RWTH Aachen University, Aachen.
Leckie, D.A., Kalkreuth, W.D., Snowdon, L.R., (1988) Source rock potential and thermal maturity of Lower Cretaceous strata; Monkman Pass area, British Columbia. *AAPG Bulletin*, 72(7), 820-838.
Lomnitz, C., (2004) Major earthquakes of Chile; a historical survey, 1535-1960. *Seismological Research Letters*, 75(3), 368-378.
Lopatin, N.V., (1971) Temperature and geologic time as factors in coalification. *Izvestiya Akademii Nauk SSSR. Seriya Geologicheskaya*, 3, 95-106.
Lutz, R., Littke, R., Gerling, P., Bonnemann, C., (2004) 2D numerical modelling of hydrocarbon generation in subducted sediments at the active continental margin of Costa Rica. *Marine and Petroleum Geology*, 21(6), 753-766.
Melnick, D., Bookhagen, B., Echtler, H., Strecker, M., (2006) Coastal deformation and great subduction earthquakes, Isla Santa María, Chile (37°S). *GSA Bulletin*, 118(11/12), 1463-1480.
Melnick, D., Bookhagen, B., Strecker, M.R., Echtler, H.P., (2009) Segmentation of megathrust rupture zones from fore-arc deformation patterns over hundreds to millions of years, Arauco peninsula, Chile. *Journal of Geophysical Research-Solid Earth*, 114.
Melnick, D., Echtler, H., (2006a) Inversion of forearc basins in southcentral Chile caused by rapid glacial age trench fill. *Geology*, 34(9), 709-712.
Melnick, D., Echtler, H., (2006b) Morphotectonic and geologic digital map compilations of the south-central Andes (36°–42°S). In: O. Oncken, G. Chong, G. Franz, P. Giese, H.-J. Götze, V.A. Ramos, M. Strecker, P. Wigger (Eds.), *The Andes—Active subduction orogeny*, *Frontiers in Earth Sciences* (Ed. by O. Oncken, G. Chong, G. Franz, P. Giese, H.-J. Götze, V.A. Ramos, M. Strecker, P. Wigger), pp. 565–568. Springer-Verlag, Berlin Heidelberg New York.
Micksch, U., (2008) The Chilean subduction zone at 38.2° S. In: *Department of Earth Sciences, Dr.*, pp. 280. Freie Universität Berlin, Berlin.
Mordojovich, C., (1981) Sedimentary basins of Chilean Pacific offshore. In: *Symposium on energy resources of the Pacific region, 12* (Ed. by M.T. Halbouty), pp. 63-82. AAPG Studies in Geology, Honolulu, HI, United States.
Müller, R.D., Roest, W.R., Royer, J.-Y., Gahagan, L.M., Sclater, J.G., (1997) Digital isochrons of the world's ocean floor. *Journal of Geophysical Research*, 102(B2), 3211-3214.
Nielsen, S.N., Glodny, J., (2006) The Middle Miocene Climate Optimum in Central and Southern Chile: 87SR/86SR Isotope Strtatigraphy on Warm-Water Mollusks. In: *XI Congreso Geológico Chileno*, Antofagasta, Chile.
Oleskevich, D., Hyndman, R., Wang, K., (1999) The updip and downdip limits to great subduction earthquakes: Thermal and structural models of Cascadia, south Alaska, SW Japan, and Chile. *J. Geophys. Res.*, 104(B7), 14965-14991.
Pardo-Casas, F., Molnar, P., (1987) Relative motion of the Nazca (Farallon) and South American plates since Late Cretaceous time. *Tectonics*, 6(3), 233-248.
Parsons, B., Sclater, J.G., (1977) An analysis of the variation of ocean floor bathymetry and heat flow with age. *Journal of Geophysical Research*, 82(5), 803-827.

Petersen, H.I., (2006) The petroleum generation potential and effective oil window of humic coals related to coal composition and age. *International Journal of Coal Geology*, 67(4), 221-248.
Pineda, V., (1983) Evolución Paleogeograáfica de la Cuenca Sedimentaria Cretácico-Terciaria de Arauco. In: J. Frutos, R. Oyarzún, M. Pincheira (Eds.), *Geología y recursos minerales de Chile* (Ed. by J. Frutos, R. Oyarzún, M. Pincheira). Editorial de la Universidad de Concepción, Concepción, Chile.
Planiglobe, (2007) Map Server. http://www.planiglobe.com.
Radic, J.P., Alvarez, P., Rojas, L., (2006) Tectonostratigraphic Evolucion of the Arauco-Itala Forearc Basin, Chile Central. SIPETROL S.A., Santiago, Chile.
Rehak, K., Strecker, M.R., Echtler, H.P., (2008) Morphotectonic segmentation of an active forearc, 37[degree sign]-41[degree sign]S, Chile. *Geomorphology*, 94(1-2), 98-116.
Rullkötter, J., Leythaeuser, D., Horsfield, B., Littke, R., Mann, U., Muller, P.J., Radke, M., Schaefer, R.G., Schenk, H.J., Schwochau, K., Witte, E.G., Welte, D.H., (1988) Organic matter maturation under the influence of a deep intrusive heat source: A natural experiment for quantitation of hydrocarbon generation and expulsion from a petroleum source rock (Toarcian shale, northern Germany). *Organic Geochemistry*, 13(4-6), 847-856.
Sánchez, M., (2004) Evolución tectónica de Isla Mocha (38°20´S;73°55´W): Configuración de un sistema anómalo en el margen occidental de la cuenca de antearco de Arauco. In: *Departamento Ciencias de la Tierra*, pp. 108. Universidad de Concepción, Concepción.
Scheidt, G., Littke, R., (1989) Comparative organic petrology of interlayered sandstones, siltstones, mudstones and coals in the Upper Carboniferous Ruhr Basin, Northwest Germany, and their thermal history and methane generation. *International Journal of Earth Sciences*, 78(1), 375-390.
Senglaub, Y., Littke, R., Brix, M.R., (2006) Numerical modelling of burial and temperature history as an approach for an alternative interpretation of the Bramsche anomaly, Lower Saxony Basin. *International Journal of Earth Sciences*, 95(2), 204-224.
Stach, E., Mackowsky, M.T., Teichmüller, M., Taylor, G.H., Chandra, D., Teichmueller, R., (1982) *Stach's textbook of coal petrology*. E. Schweizerbart'sche Verlagsbuchhandlung, Stuttgart.
Sweeney, J., Burnham, A.K., (1990) Evaluation of a simple model of vitrinite reflectance based on chemical kinetics. *AAPG Bulletin*, 74(10), 1559-1570.
Sykes, R., Snowdon, L.R., (2001) Guidelines for assessing the petroleum potential of coaly source rocks using Rock-Eval pyrolysis. In: *20th International Meeting on Organic Geochemistry*, pp. 1441-1455, Nancy, France.
Taylor, G.H., Teichmueller, M., Davis, A., Diessel, C.F.K., Littke, R., Robert, P., Glick, D.C., Smyth, M., Swaine, D.J., Vanderbroucke, M., Espitalie, J., (1998) *Organic petrology*. Gebrueder Borntraeger, Berlin.
Teichmüller, M., (1987) Organic material and very low-grade metamorphism. In: M. Frey (Ed.), *Low Temperature Metamorphism* (Ed. by M. Frey), pp. 114-161. Blackie Academic & Professional, Glasgow.
Teichmüller, M., Durand, B., (1983) Fluorescence microscopical rank studies on liptinites and vitrinites in peat and coals, and comparison with results of the rock-eval pyrolysis. *International Journal of Coal Geology*, 2(3), 197-230.
Tissot, B.P., Welte, D.H., (1984) *Petroleum formation and occurrence*. Springer, Berlin.
Van Hinte, J.E., (1978) Geohistory analysis; application of micropaleontology in exploration geology. *AAPG Bulletin*, 62(2), 201-222.
vanKrevelen, D.W., (1961) *Coal; typology, physics, chemistry, constitution*. Elsevier, Amsterdam.

Wang, C.Y., Liang, G.P., Shi, Y.L., (1993) Heat-Flow Across the Toe of Accretionary Prisms - The Role of Fluid Flux. *Geophysical Research Letters*, 20(8), 659-662.
Waples, D.W., (1980) Time and temperature in petroleum formation; application of Lopatin's method to petroleum exploration. *AAPG Bulletin*, 64(6), 916-926.
Welte, D.H., Yükler, M.A., (1981) Petroleum origin and accumulation in basin evolution; a quantitative model. *AAPG Bulletin*, 65(8), 1387-1396.
Wenzel, O., (1969) Geologiá, Reservas y Pertrografia de los Carbones Chilenos, *El Carbón la Siderurgia Latinoamericana*, pp. 173-193. Seminario ILAFA, Santiago.
Wenzel, O., (1972) Geología y reservas del yacimiento carbonífero de Lebu. Empresa Nacional del Carbón S.A., unpublished.
Wenzel, O., Wathelet, J., Chávez, L., Bonilla, R., (1975) La sedimentación cíclica Meso-Cenozoica en la región Carbonífera de Arauco-Concepción, Chile. In: *Anales del 2º Congreso Americano de Geología Económica*, pp. 215-237, Buenos Aires.
Wheeler, H.E., (1958) Time-stratigraphy. *AAPG Bulletin*, 42(5), 1047-1063.
Wygrala, B., (1989) Integrated study of an oil field in the southern Po-basin, North Italy. In: *Forschungszentrum Jülich*. Universität Köln, Jülich.

Table 1: Results of the vitrinite reflectance measurements (Kuhn, 2007)

Sample Number	Well Name or Source	Formation (Sample Information)	Sample Depth in Well [m]	VRr [%]	Standard Deviation [%]	Number of Reading
06/168	Mine Trongol	Curanilahue (Coal)		0.52	0.026	303
06/170	Mine Trongol	Curanilahue (Coal)		0.50	0.024	314
06/174	Mine Fortuna, Lebu	Trihueco (Coal)		0.52	0.025	106
06/177	Mine Fortuna, Lebu	Trihueco (Coal)		0.65	0.021	106
06/182	Pirquen Sanzana, Lebu	Trihueco (Coal)		0.65	0.026	210
06/184	Yoville, Chile	Curanilahue (Coal)		0.58	0.028	108
06/185	Arauco,Chile	Ranquil (Coal)		0.41	0.028	100
06/186	Arauco,Chile	Ranquil (Coal Fragments)		0.51	0.029	100
06/189	NW of Arauco Peninsula	Trihueco (Coal Fragments)		0.67	0.057	109
06/191	SE of Curanilahue	Curanilahue (Coal)		0.63	0.028	320
07/001	Curanilahue-1	Quiriquina (Core)	979	0.92	0.052	100
07/002	Curanilahue-1	Quiriquina (Core)	1055	0.94	0.053	100
07/005	Curanilahue-2	Quiriquina (Core)	1521	0.74	0.032	90
07/006	Curanilahue-2	Quiriquina (Core)	1521	0.74	0.035	100
07/008	Curanilahue-2	Quiriquina (Core)	1536	0.74	0.034	100
07/009	Curanilahue-2	Quiriquina (Core)	1536	0.76	0.035	100
07/010	Curanilahue-2	Quiriquina (Core)	1521	0.73	0.029	114
07/014	Rio Trongol-1	Boca Lebu (Core)	277	0.69	0.036	100
07/015	Rio Trongol-1	Boca Lebu (Core)	277	0.69	0.033	85
07/016	Rio Trongol-1	Quiriquina (Core)	881	0.83	0.044	104
07/018	Tubul-1	Trihueco (Core)	1066	0.72	0.048	246
07/019	Tubul-1	Trihueco (Core)	1066	0.74	0.070	94
07/021	Tubul-1	Curanilahue (Core)	1610	0.82	0.037	209
07/022	Tubul-1	Curanilahue (Core)	1614	0.82	0.036	100
07/023	Tubul-1	Quiriquina (Core)	2047	0.90	0.041	100
07/024	Tubul-1	Quiriquina (Core)	2139	0.92	0.051	100
07/025	Tubul-1	Quiriquina (Core)	2186	0.95	0.039	54
07/026	Tubul-1	Quiriquina (Core)	2186	0.93	0.039	72
07/027	Tubul-1	Quiriquina (Core)	2186	0.94	0.053	100
07/030	Tubul Este-1	Curanilahue (Core)	1109	0.82	0.032	87
07/031	Tubul Este-1	Curanilahue (Core)	1146	0.79	0.035	97
07/033	Lebu-1	Quiriquina (Core)	1125	0.85	0.056	102
07/034	Lebu-4	Quiriquina (Core)	1702	0.90	0.034	20
07/035	Lebu-5	Quiriquina (Core)	1054	0.84	0.038	100
07/036	Lebu-5	Quiriquina (Core)	1054	0.85	0.046	62
07/037	Lebu-5	Quiriquina (Core)	1449	0.96	0.051	100
07/038	Lebu-5	Quiriquina (Core)	1620	1.00	0.063	100
07/040	Lebu-6	Quiriquina (Core)	1793	0.92	0.036	32
07/042	Penhue-1	Millongue (Core)	633	0.61	0.098	100
07/043	Penhue-1	Trihueco (Core)	878	0.67	0.037	100
07/044	Penhue-1	Trihueco (Core)	1039	0.73	0.036	203
07/045	Penhue-1	Trihueco (Core)	1051	0.68	0.038	200
07/046	Penhue-1	Trihueco (Core)	1057	0.68	0.026	112
07/047	Penhue-1	Trihueco (Core)	1062	0.65	0.033	253
07/048	Penhue-1	Trihueco (Core)	1067	0.69	0.035	274
07/049	Penhue-1	Trihueco (Core)	1072	0.69	0.034	266
07/050	Penhue-1	Quiriquina (Core)	1501	0.85	0.061	8
07/051	Penhue-1	Quiriquina (Core)	1704	0.89	0.061	100
07/052	Penhue-1	Quiriquina (Core)	1704	0.91	0.061	120
07/053	Penhue-1	Quiriquina (Core)	1859	0.93	0.051	102
07/054	Penhue-1	Quiriquina (Core)	1930	0.96	0.064	51

Table 2: Results of pyrolysis: Total organic carbon (TOC), total inorganic carbon (TIC) measurements and Rock-Eval pyrolysis from Kuhn (2007)

Sample Number	Well Name or Source	Formation	S1 [mg/g rock]	S2 [mg/g rock]	S3 [mg/g rock]	Tmax [°C]	OI [mg CO_2/ gTOC]	HI [mg HC/ gTOC]	PI [-]	TOC [%]	TIC [%]
06/168	Mine Trongol	Curanilahue	8.70	226.34	1.68	424	3	395	0.04	57.24	0.19
06/170	Mine Trongol	Curanilahue	5.45	272.34	5.94	428	8	378	0.02	72.11	0.30
06/174	Mine Fortuna, Lebu	Trihueco	20.14	239.48	3.33	421	5	356	0.08	67.36	0.22
06/177	Mine Fortuna, Lebu	Trihueco	3.92	228.81	7.56	425	10	294	0.02	77.79	0.23
06/182	Pirquen Sanzana, Lebu	Trihueco	2.45	202.15	5.24	422	7	273	0.01	74.09	0.27
06/183	Pirquen Sanhueza, Lebu	Trihueco	1.79	79.53	38.52	424	62	127	0.02	62.38	0.41
06/184	Yoville, Chile	Curanilahue	2.87	203.44	4.65	425	6	274	0.01	74.36	0.08
06/185	Arauco,Chile	Ranquil	0.43	2.98	17.40	409	79	14	0.12	21.93	0.04
06/186	Arauco,Chile	Ranquil	0.35	11.66	1.74	425	23	157	0.03	7.43	0.16
06/190	Colico Norte, Chile	Curanilahue	10.16	293.70	6.37	421	9	404	0.03	72.69	0.07
06/191	SE of Curanilahue	Curanilahue	2.70	148.86	4.18	423	7	256	0.02	58.13	0.16
07/001	Curanilahue-1	Quiriquina	0.07	0.23	0.06	442	10	38	0.22	0.60	0.04
07/002	Curanilahue-1	Quiriquina	0.05	0.11	0.08	431	15	22	0.30	0.50	0.18
07/004	Curanilahue-2	Quiriquina	0.04	0.07	0.02	437	11	46	0.38	0.14	0.12
07/005	Curanilahue-2	Quiriquina	0.21	0.58	0.35	439	22	37	0.26	1.56	0.06
07/006	Curanilahue-2	Quiriquina	0.23	0.66	0.47	437	26	37	0.26	1.78	0.09
07/008	Curanilahue-2	Quiriquina	0.36	1.10	0.08	428	4	53	0.25	2.08	0.20
07/009	Curanilahue-2	Quiriquina	0.51	3.08	0.15	435	3	54	0.14	5.69	0.12
07/010	Curanilahue-2	Quiriquina	1.32	7.91	0.77	443	7	72	0.14	11.04	0.13
07/014	Rio Trongol-1	Boca Lebu	0.07	0.25	0.20	433	26	33	0.21	0.76	0.04
07/015	Rio Trongol-1	Boca Lebu	0.10	0.18	0.14	433	25	34	0.33	0.53	0.06
07/016	Rio Trongol-1	Quiriquina	0.04	0.16	0.06	433	14	39	0.21	0.38	0.03
07/018	Tubul-1	Trihueco	0.03	0.35	0.29	436	29	35	0.07	0.99	1.34
07/019	Tubul-1	Trihueco	0.07	0.24	0.17	435	17	24	0.21	1.00	0.02
07/021	Tubul-1	Curanilahue	0.19	1.45	0.66	428	14	32	0.12	4.53	0.04
07/022	Tubul-1	Curanilahue	0.09	0.69	0.13	443	12	66	0.12	1.04	0.70
07/023	Tubul-1	Quiriquina	0.04	0.16	0.27	437	71	42	0.18	0.38	2.36
07/026	Tubul-1	Quiriquina	0.06	0.17	0.03	432	5	36	0.27	0.48	0.09
07/027	Tubul-1	Quiriquina	0.02	0.11	0.00	436	0	31	0.18	0.36	0.08
07/031	Tubul Este-1	Curanilahue	0.05	0.22	0.33	449	56	37	0.19	0.58	0.02
07/033	Lebu-1	Quiriquina	0.27	0.58	0.44	424	27	36	0.31	1.63	0.13
07/034	Lebu-4	Quiriquina	0.08	0.05	0.13	437	68	26	0.57	0.19	0.18
07/036	Lebu-5	Quiriquina	0.13	0.47	0.00	427	0	47	0.21	0.99	0.09
07/038	Lebu-5	Quiriquina	0.09	0.19	0.23	438	33	27	0.31	0.70	0.11
07/040	Lebu-6	Quiriquina	0.04	0.05	0.24	433	98	21	0.41	0.24	0.04
07/041	Penhue-1	Ranquil	0.08	0.27	1.55	422	129	23	0.22	1.20	0.32
07/042	Penhue-1	Millongue	0.04	0.03	0.59	415	174	9	0.57	0.34	0.01
07/044	Penhue-1	Trihueco	0.12	1.23	0.20	434	20	121	0.09	1.02	0.16
07/046	Penhue-1	Trihueco	0.29	5.37	0.45	431	13	151	0.05	3.56	0.12
07/051	Penhue-1	Quiriquina	0.24	0.55	0.22	437	15	37	0.30	1.47	0.09
07/053	Penhue-1	Quiriquina	0.05	0.09	0.23	431	61	22	0.37	0.38	0.16
07/054	Penhue-1	Quiriquina	0.04	0.14	0.17	447	30	25	0.23	0.55	0.37

Table 3: List of lithologies used during numerical modelling for the formations of the Arauco Basin. Physical parameters are based on the default lithology parameters that are defined in PetroMod 10

Formation	Clay	Clay/Silt	Silt	Sand	Limestone	Coal	Basement	Matrix Density	Matrix thermal conductivity		Matrix Heat Capacity	
	% of complete rock							[kg/m³]	@ 20°C [W/m/K]	@ 100°C [W/m/K]	@ 20°C [kcal/kg/K]	@ 100°C [kcal/kg/K]
Quaternary		15	10	75				2717.0	3.28	2.91	0.206	0.238
Tubul	55	4	17	24				2708.2	2.20	2.12	0.207	0.240
Miocene Turbidite		15	15	70				2717.0	3.17	2.84	0.206	0.239
LowMio	10		79.6	10		0.4		2713.5	2.14	2.07	0.215	0.249
Oligocene	10	15	35	40				2715.0	2.56	2.39	0.209	0.242
Millongue	18	44	38					2707.6	2.38	2.27	0.205	0.237
Trihueco		9	14	74		3		2684.6	3.09	2.82	0.209	0.242
BocaLebu	10	77	12		1			2702.7	1.79	1.81	0.207	0.240
Curanilahue	1	15	39	44		1		2705.6	2.65	2.46	0.210	0.243
Quiriquina	1	29	49	20	0.6	0.4		2709.6	2.23	2.14	0.211	0.244
Basement							100	2750.0	2.72	2.35	0.188	0.223

Table 4: Data of the conceptual models of the Miocene scenario for well “Penhue 1”

Formation	End of Formation in Well [m]	Thickness [m]		Age of Deposition Before Present [Myr]		Age of Erosion Before Present [Myr]		Used Lithology
		Preserved	Eroded	from	till	from	till	
Tubul	73	73	10	2.59	1.8	1.8	0.0	Rock Tubul
Sub+Inv	73	0	2500	12.6	7.5	5.0	3.6	Rock Turbidite
LowMio	458	385	600	15.5	12.6	3.6	2.6	Rock LowMio
E M LowMio	458	0	60	21.0	18.0	18.0	16.0	Rock LowMio
Oligocene	458	0	60	33.0	28.0	28.0	26.0	Rock Oligocene
Millongue	691	233	117	39.0	33.9	26.0	22.0	Rock Millongue
Triheco	1141	450		44.0	39.0			Rock Trihueco
Boca Lebu	1295	154		50.0	44.0			Rock BocaLebu
Curanilahue	1502	207		57.0	50.0			Rock Curanilahue
Quiriquina	1962	460	140	84.0	70.0	70.0	65.5	Rock Quiriquina
Paleozoic	16962	15000		200.0	150.0			BASEMENT

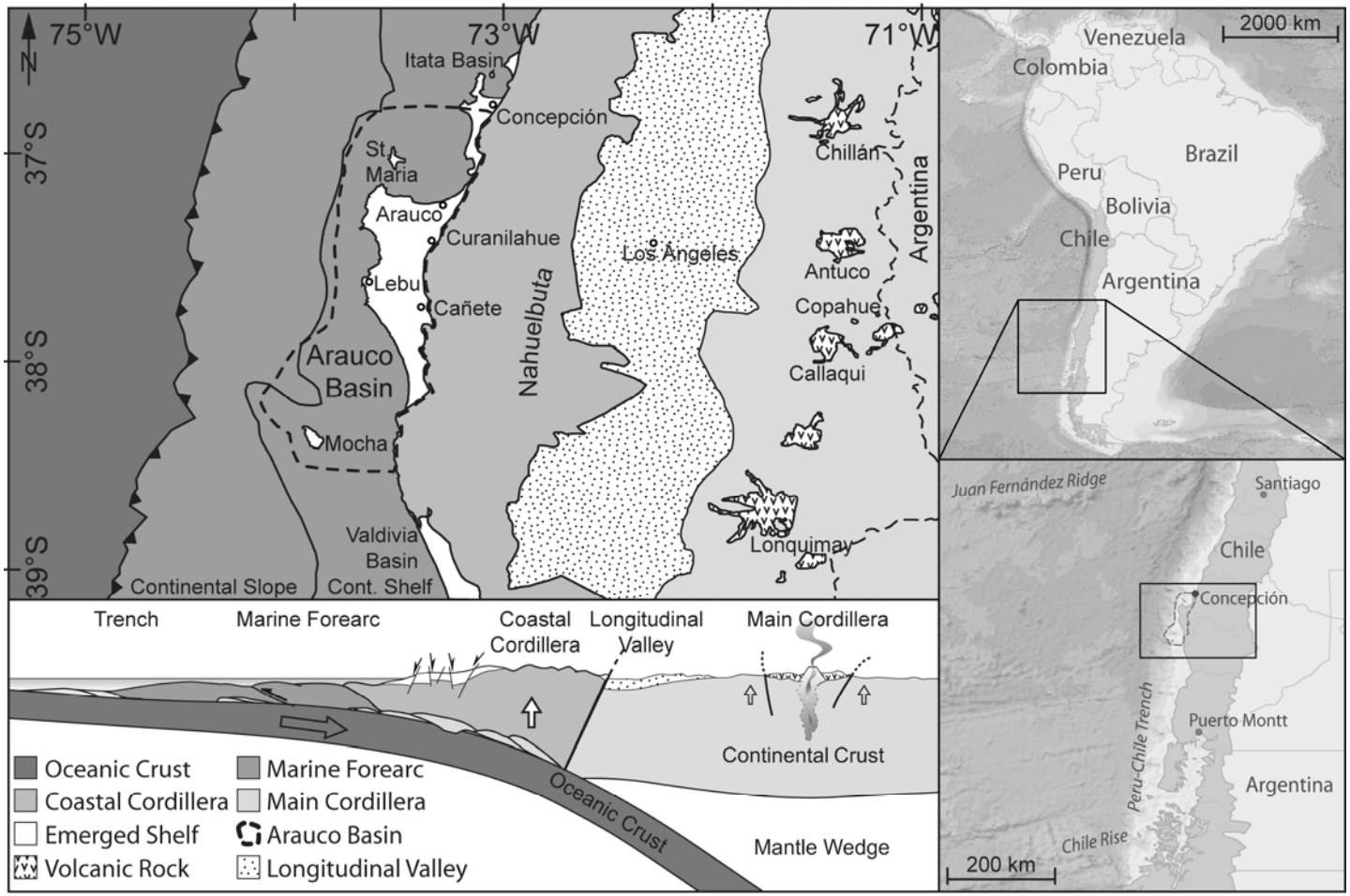

Fig. 1: The maps on the right show the location of the Arauco basin in its position east of the Peru-Chile Trench in the forearc of the South America Plate south of Concepción (Planiglobe, 2007); the left simplified geological map shows the main structures surrounding the emerged Arauco forearc basin (after Melnick & Echtler (2006b)) together with the schematic profile indicating the elevation of the important features of the arc complex from the trench to the volcanic arc

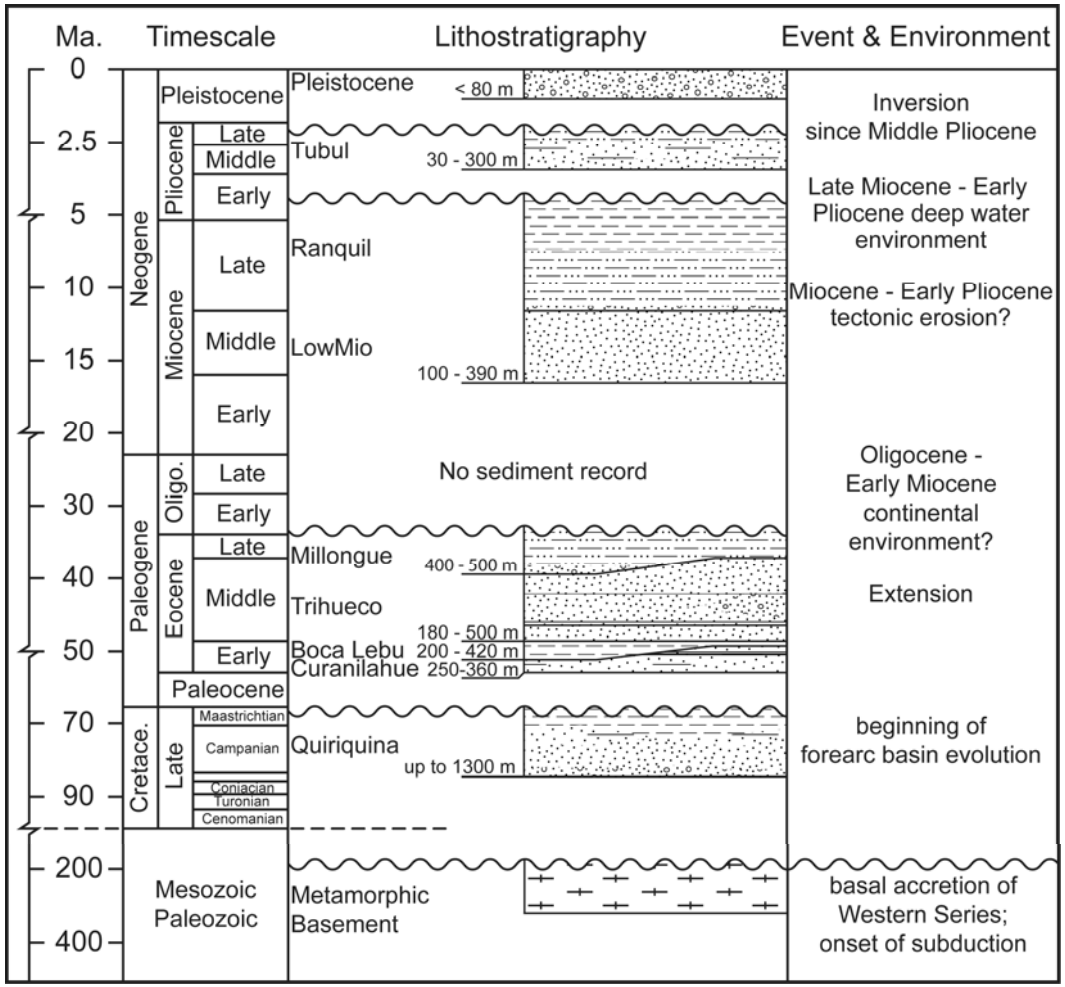

Fig. 2: Generalized stratigraphy of preserved sediments in the Arauco basin based on well descriptions from ENAP using the International Geologic Time Scale after Gradstein *et al*. (2004); legend for sediment patterns is given in Fig. 3

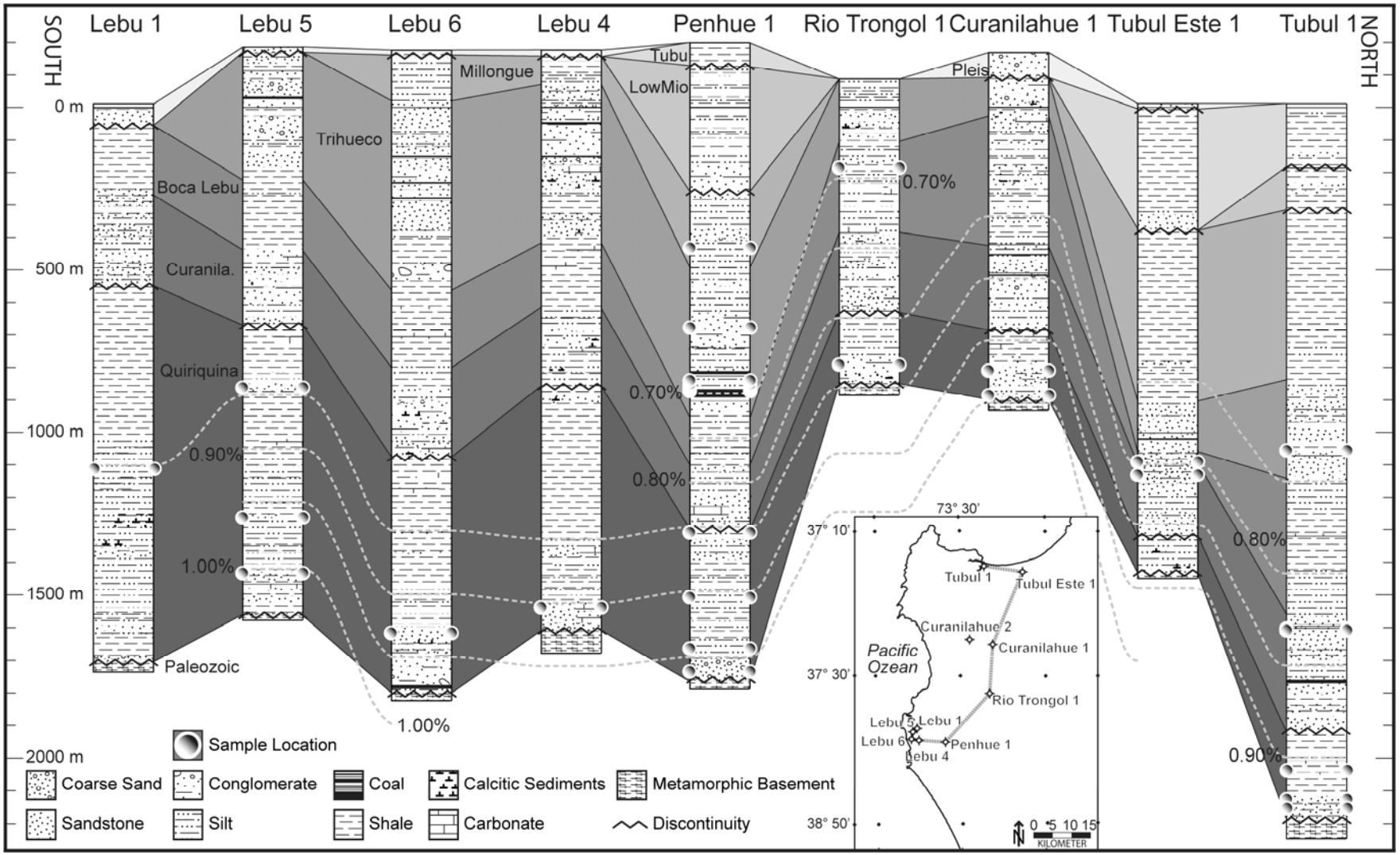

Fig. 3: Correlation of the major stratigraphic units of 9 of the sampled wells (supplied by ENAP) along the grey line in the small location map of the Arauco basin at the bottom.

Light grey isolines show interpolated VR_r values based on new data derived from core samples.

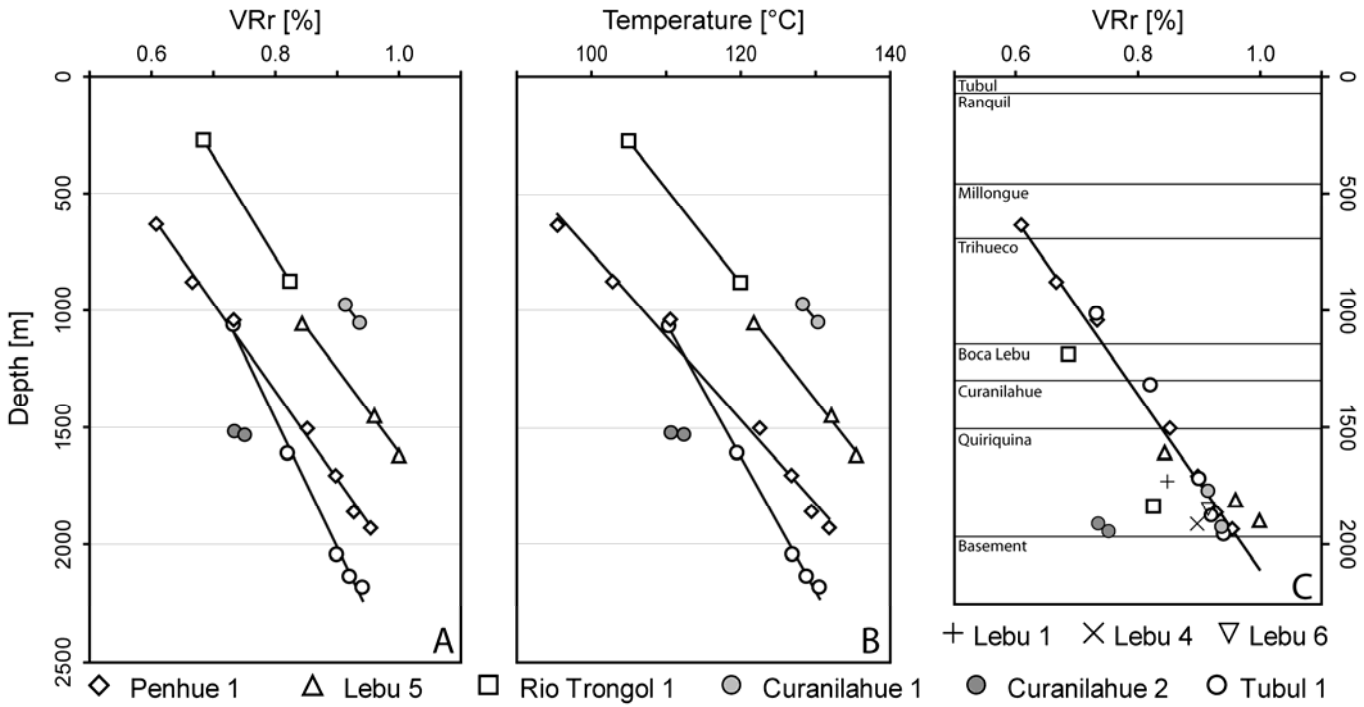

Fig. 4: Graph A indicates the VR_r data against depth of all wells with data at more than one measured depth point; when using Formula 1 together with the data in A it is possible to define the temperature gradients during a long termed temperature maximum in the basins sediment as displayed in Graph B. Graph C shows the VR_r data measured on drill core samples of nine wells of the Arauco basin. The data of seven wells are standardised to their stratigraphic position to the well “Penhue 1”. The displayed data of the wells fit well with a linear gradient and therefore suggest a similar temperature history. Since the overall trend does not show significant anomalies in any direction, it can be concluded that the maximum temperature event occurred after the youngest of the measured samples was deposited. Since the youngest drill core sample on which VR_r was measured is from the Millongue Formation (Upper Eocene), an Upper Eocene or younger maximum temperature event is evident.

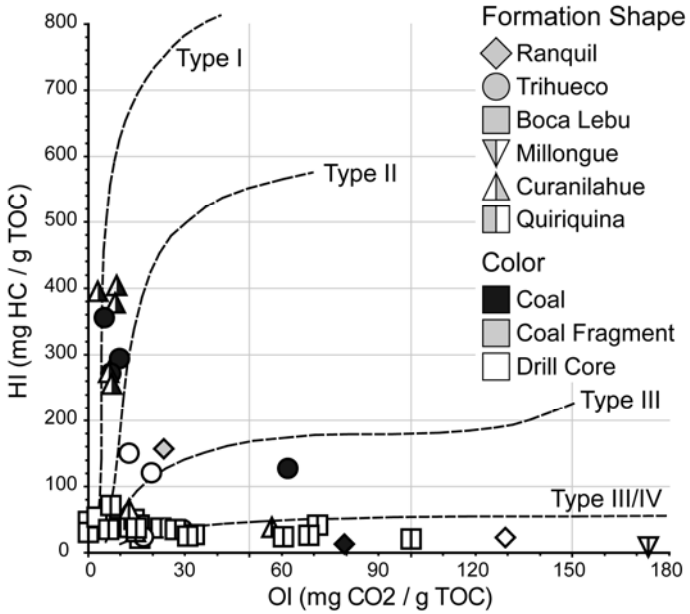

Fig. 5: Van-Krevelen-Type-Diagram with HI and OI from Table 2 of all Arauco Peninsula samples tested. The clustering of the coal samples parallel to the HI axis is similar to Cretaceous and Paleogene coals in New Zealand and South-East Asia.

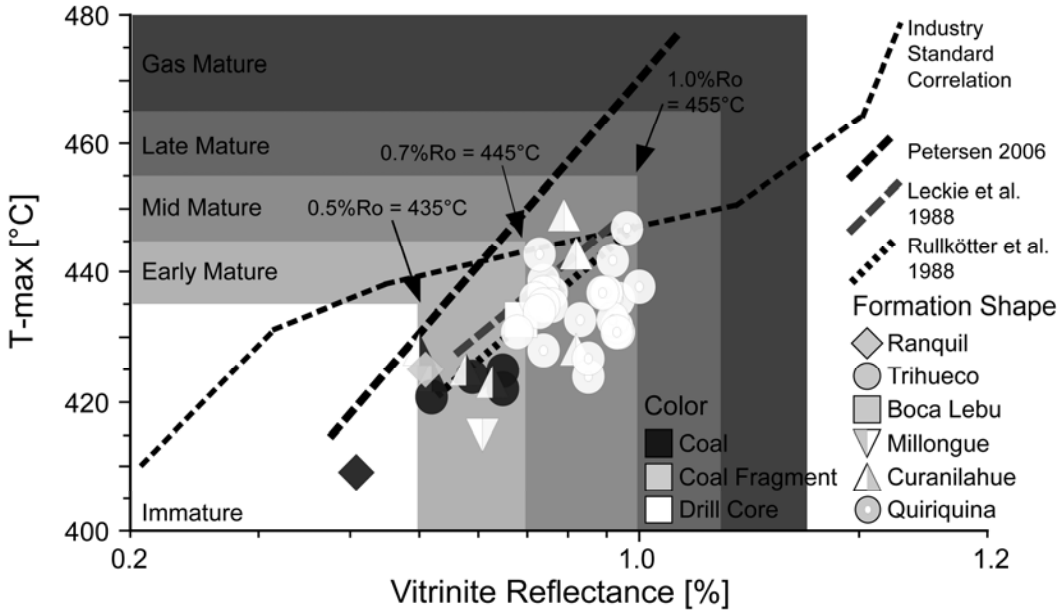

Fig. 6: Plot of VR_r (Table 1) versus T_{max} (Table 2) shows reasonable correlation between both thermal maturity indicators. Superimposed are values from Leckie *et al.* (1988), the Posidonia Shale taken form Rullkötter *et al.* (1988) and a worldwide database (Petersen, 2006) for comparison.

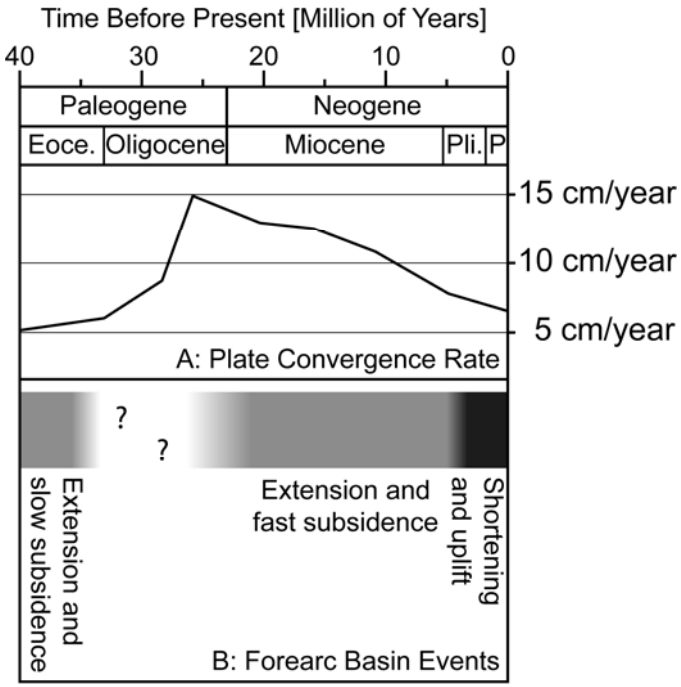

Fig. 7: Tectonics that influence the development of the basin, which need to be incorporated into the conceptual model. A indicates the convergence velocity of the Nazca Plate and the South American Continent in the last 40 Myr, while B depicts the internal development stages of the basin (both based on Melnick & Echtler (2006a) and references within).

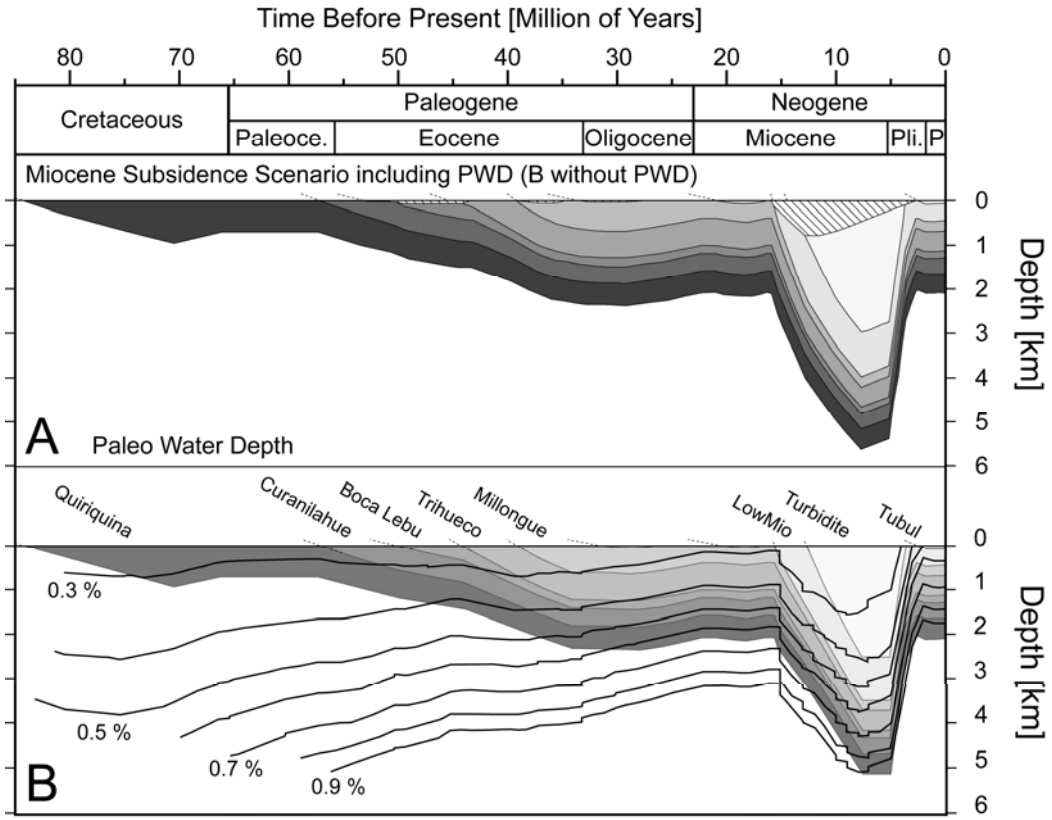

Fig. 8: Graphic presentation of the conceptual models for well “Penhue 1” for the Miocene subsidence scenario described in Table 4; A includes the PWD while only the rock column is displayed in B. Calculated VR_R values are indicated in B.

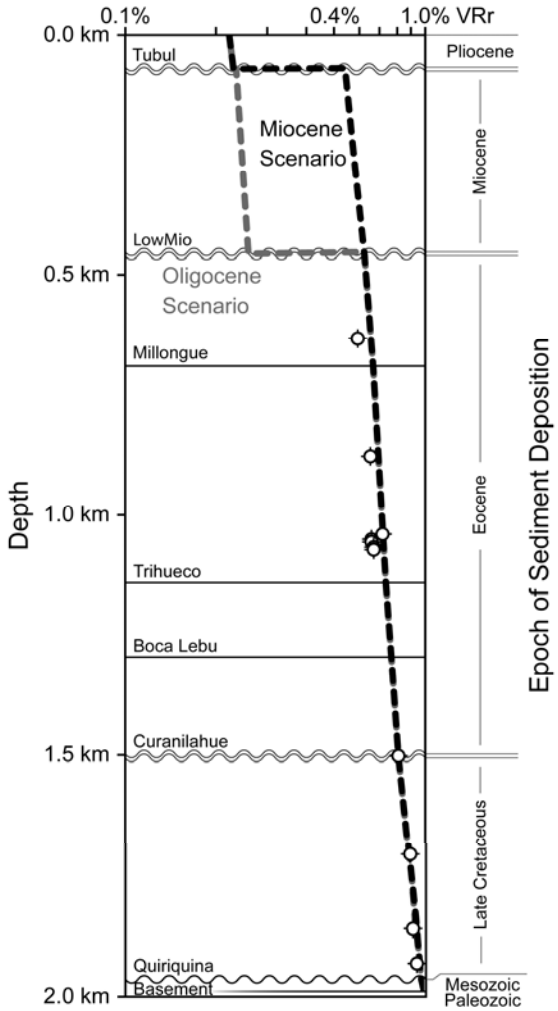

Fig. 9: VR_r data fit of the Oligocene (structural inversion and erosion 3120 m and HF of 64.7 mW/m²) and Miocene (3100 m and 64.5 mW/m²) structural inversion and erosion model using the conceptual model described in Table 4 (modifications were made for the Oligocene scenario).

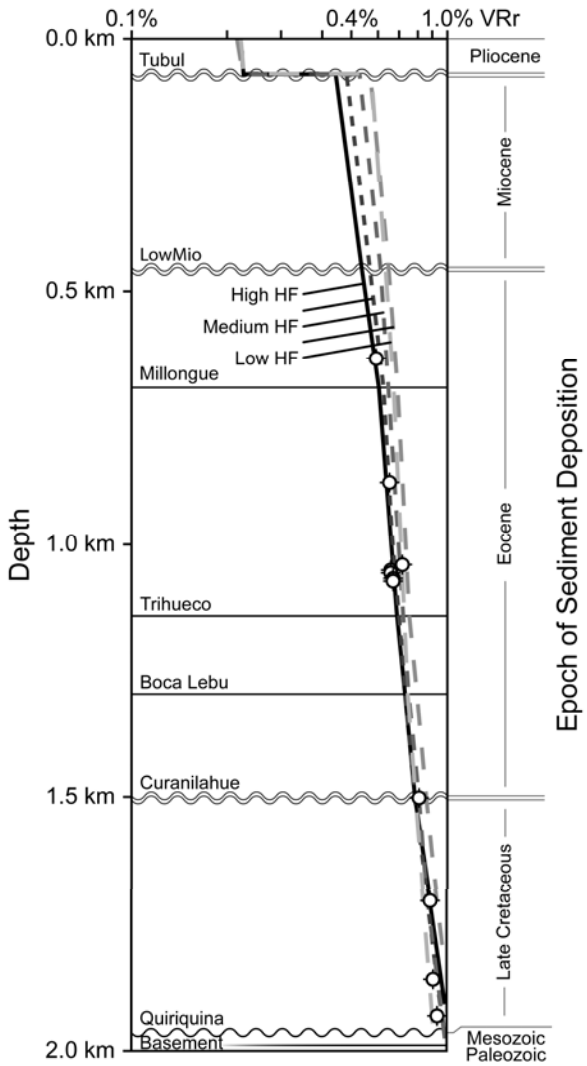

Fig. 10: Different results for modelling approaches for “Penhue 1” with different HF values and the structural inversion and erosion combination as displayed in Figure 11

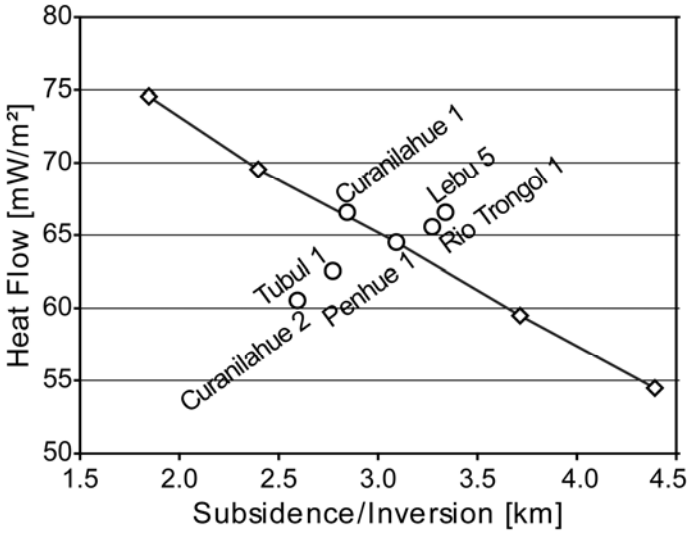

Fig. 11: Diamond shape symbols show different combinations of HF values and the structural inversion and erosion required for the most reasonable fit with calibration data set of “Penhue 1” as displayed in Figure 10; circles indicate best fit models for all tested wells with two or more calibration points

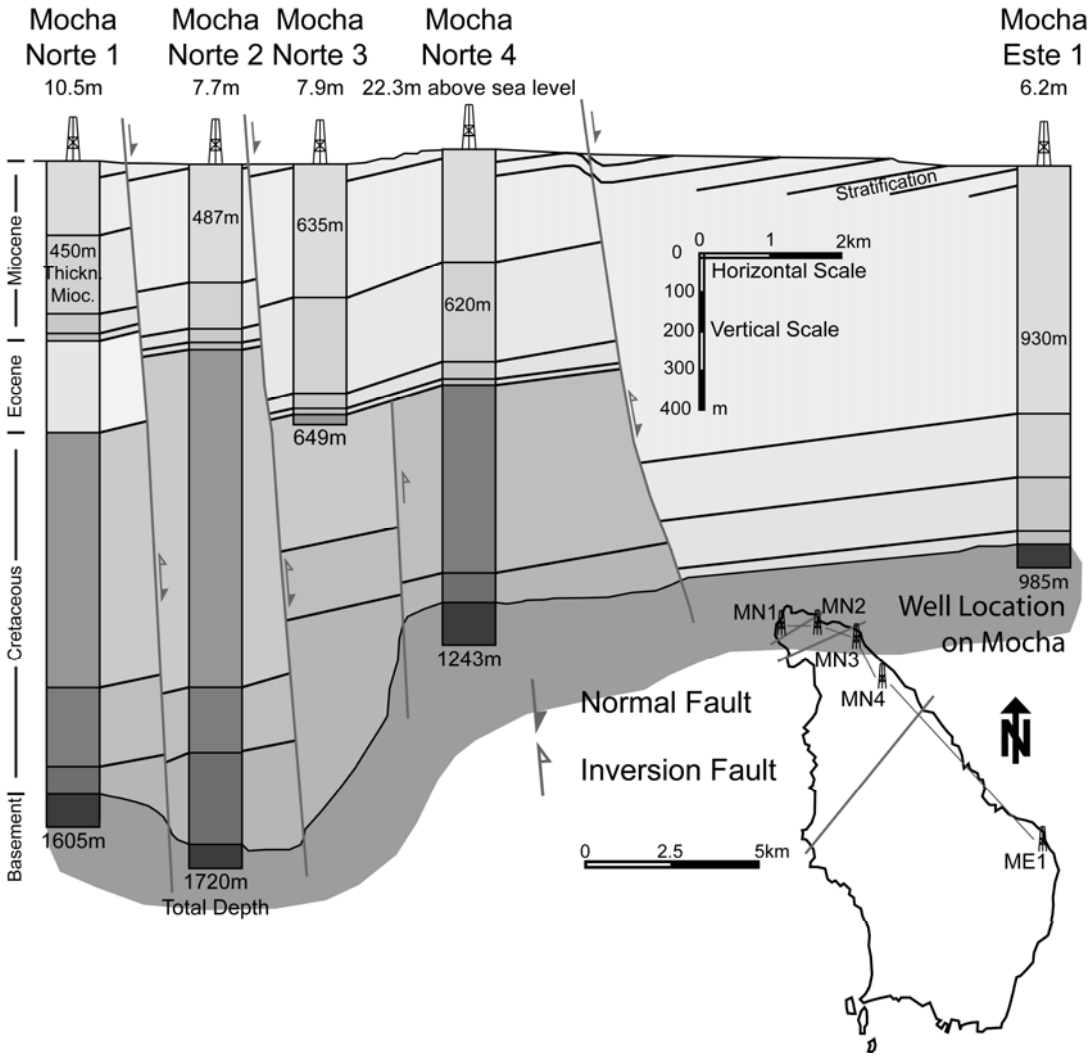

Fig. 12: Stratigraphic correlation of the formations in wells drilled on Isla Mocha by ENAP

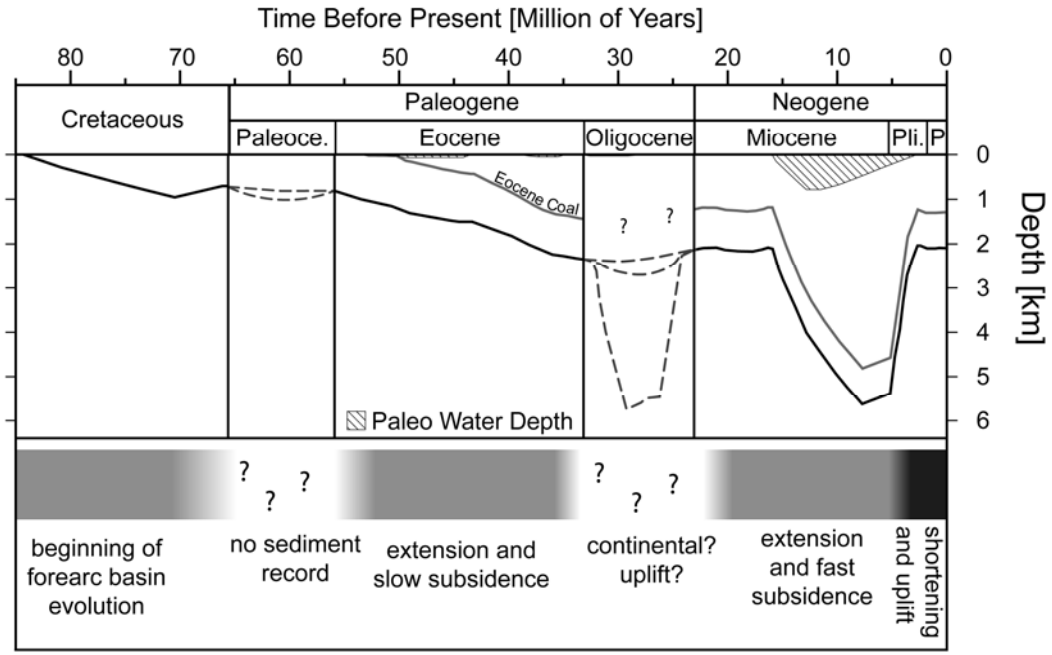

Fig. 13: Possible development of the subsidence and inversion history of the Arauco basin is displayed for the Miocene inversion scenario by the black line. The diagonally striped areas represent the PWD through time. Areas of unavailable sediment record in the greater area are marked by lighter areas in the bottom part of the figure. For these times the dashed grey lines represent possible scenarios how the basement –sediment contact could have developed; greater and lesser vertical movements are described. The grey line represents the Eocene coal layer from which several samples were derived.